An asymptotic homogenization approach to the microstructural evolution of heterogeneous media

Original
An asymptotic homogenization approach to the microstructural evolution of heterogeneous media / Ramírez-Torres, Ariel; Di Stefano, Salvatore; Grillo, Alfio; Rodríguez-Ramos, Reinaldo; Merodio, José; Penta, Raimondo. - In: INTERNATIONAL JOURNAL OF NON-LINEAR MECHANICS. - ISSN 0020-7462. - 106:(2018), pp. 245-257. [10.1016/j.ijnonlinmec.2018.06.012]

Availability:
This version is available at: 11583/2720458 since: 2020-06-03T17:41:57Z

Publisher:
Elsevier Ltd

Published
DOI:10.1016/j.ijnonlinmec.2018.06.012

An Asymptotic Homogenization Approach to the Microstructural Evolution of Heterogeneous Media

Ariel Ramírez-Torres[a], Salvatore Di Stefano[a], Alfio Grillo[a], Reinaldo Rodríguez-Ramos[b], José Merodio[c], Raimondo Penta[d,*]

[a]*Dipartimento di Scienze Matematiche "G. L. Lagrange", Politecnico di Torino, Torino, 10129, Italy*
[b]*Departamento de Matemáticas, Facultad de Matemática y Computación, Universidad de La Habana, La Habana, CP 10400, Cuba*
[c]*Departamento de Mecánica de los Medios Continuos y T. Estructuras, E.T.S. de Caminos, Canales y Puertos, Universidad Politécnica de Madrid, Madrid, CP 28040, Spain*
[d]*School of Mathematics and Statistics, Mathematics and Statistics Building, University of Glasgow, University Place, Glasgow G12 8QQ, UK*

Abstract

In the present work, we apply the asymptotic homogenization technique to the equations describing the dynamics of a heterogeneous material with evolving micro-structure, thereby obtaining a set of upscaled, effective equations. We consider the case in which the heterogeneous body comprises two hyperelastic materials and we assume that the evolution of their micro-structure occurs through the development of plastic-like distortions, the latter ones being accounted for by means of the Bilby-Kröner-Lee (BKL) decomposition. The asymptotic homogenization approach is applied simultaneously to the linear momentum balance law of the body and to the evolution law for the plastic-like distortions. Such evolution law models a stress-driven production of inelastic distortions, and stems from phenomenological observations done on cellular aggregates. The whole study is also framed within the limit of small elastic distortions, and provides a robust framework that can be readily generalized to growth and remodeling of nonlinear composites. Finally, we complete our theoretical model by performing numerical simulations.

Keywords: Asymptotic homogenization, heterogeneous media, remodeling, BKL decomposition, two-scale plasticity, nonlinear composites

*Corresponding author
Email address: raimondo.penta@glasgow.ac.uk (Raimondo Penta)

1. Introduction

The study of material growth, remodeling and aging is of great importance in Biomechanics, specially when the tissue, in which these processes occur, features a very complex structure, with different scales of observation and various constituents.

In the literature, the study of heterogeneous materials follows several approaches. In this work we focus on the multi-scale asymptotic homogenization technique [4, 5, 8, 14, 77], which exploits the information available at the smallest scale characterizing the considered medium or phenomenon to obtain an effective description of the medium or phenomenon itself valid at its largest scale. This is achieved by expanding in asymptotic series the equations constituting the mathematical model formulated at the lowest scale. As a result, the coefficients of the effective governing equations encode the information on the other hierarchical levels, as they are to be computed solving microstructural problems at the smaller scales. The multi-scale asymptotic homogenization approach has been successfully applied to investigate various physical systems due to its potentiality in decreasing the complexity of the problem at hand. Biomechanical applications of asymptotic homogenization may be found mainly in nanomedicine [81], biomaterials modeling, such as the bone [58, 65], tissue engineering [24], poroelasticity [63], and active elastomers [64]. Most of the literature concerning applications of the asymptotic homogenization technique focuses on linearized governing equations, as in this case it is possible to obtain, under a number of simplifying assumptions, a full decoupling between scales, which leads to a dramatic reduction in the computational complexity, as also noted for example in [64]. In fact, homogenization in nonlinear mechanics is usually tackled via average field approaches based on representative volume elements or Eshelby-based techniques (see e.g. [41] for a comparison between the latter and asymptotic homogenization), as done for example in [11]. These homogenization approaches are typically well-suited when seeking for suitable bounds for the coefficients of the model, such as the elastic moduli, while asymptotic homogenization can provide a precise characterization of the coefficients under appropriate regularity assumptions (namely, *local periodicity*).

However, to the best of our knowledge and understanding, there exists only a few examples, e.g. [15, 68, 74, 75], dealing with the asymptotic homogenization in the case of media undergoing large deformations. In [68], the static microstructural effects of periodic hyperelastic composites at finite strain are investigated. In [74], the interactions between large deforming solid and fluid media at the microscopic level are described by using the two-scale homogenization technique and the updated Lagrangian formulation. In [15], the effective equations describing the flow, elastic deformation and transport in an active poroelastic medium were obtained. Therein, the authors considered the spatial homogenization of a coupled transport and fluid-structure interaction model, incorporating details of the microscopic system and admitting finite growth and deformation at the pore scale. Some works can be also found dealing with homogenization in the case of elastic perfectly plastic constituents [79, 83].

Here we embrace the asymptotic homogenization approach and consider a heterogeneous body composed of two hyperelastic solid constituents subjected to the evolution of their internal structure. We refer to this phenomenon as to material remodeling and we interpret it with the production of plastic-like distortions. The wording "material remodeling" is used as a synonym of "evolution of the internal structure" of a tissue, and is intended in the sense of [16], who states that *"biological systems can adapt their structure [...] to accommodate a changed mechanical load environment"*. In this case, always in the terminology of [16] and [80], one speaks of *epigenetic* adaptation (or material remodeling). In the framework of the manuscript, such adaptation is assumed to occur through plastic-like distortions that represent processes like the redistribution of the adhesion bonds among the tissue cells.

It is worth to recall in which sense the concept of "plastic distortions", conceived in the context of the Theory of Plasticity (cf. e.g. [50, 55]), and originally referred to non-living materials such as metals or soils, can be imported to describe the structural evolution of biological tissues. To this end, it is important to emphasize that the wording "plastic distortions" is understood as the result of a complex of transformations that conducts to the reorganization of the internal structure of a material, and that — as anticipated in the Introduction— such reorganization is referred to as "remodeling" in the biomechanical context.

The ways in which the structural tranformations may take place in a given material depend on the structural properties of the material itself. For this reason, the plasticity in metals is markedly different from that occurring in amorphic materials. In the case of metals, indeed, for which the internal structure is granular and characterized by the arrangement of the atomic lattice within each grain, plastic distortions are the *macroscopic* manifestation of the formation and evolution of lattice defects. As reported in [55], such defects can be due, for example, to edge dislocations, wedge disclinations, missing atoms at some lattice sites, or to the presence of atoms in the lattice interstices. To describe how the defects evolve, thereby giving rise to the plastic distortions, one should compare the real lattice at the current instant of time with an ideal lattice, and decompose the overall deformation (i.e., shape change *and* structural transformation) into an elastic and an inelastic contribution [55]. The elastic contribution describes the part of deformation that is recoverable by completely relaxing mechanical stress, whereas the inelastic contribution represents the structural variation, which, in general, is of irreversible nature.

Clearly, metals have structural features markedly different from those of living matter. Still, some of the fundamental mechanisms that trigger the reorganization of their internal structure can be adapted to describe the remodeling of biological tissues.

For instance, in the case of bones, plastic-like phenomena are due to the formation of microcracks that, in turn, favors the gliding of the material along the direction of the opening of the cracks [17, 86]. Lastly, as anticipated above, in the case of biological tissues such as cellular aggregates, the phenomenon analogous to the generation of dislocations is the rearrangement of the adhesion bonds among the cells or the reorganization of the extracellular matrix due to the reorientation of the collagen fibers or their deposition and resorption, as is the case for blood vessels [48]. Also in all these situations, the comparison of the real configuration of the tissue with an "ideal" one, taken as reference, permits the separation of the overall deformation into an elastic part and a structure-related, "plastic-like" part.

Here, taking inspiration from the theory of finite Elastoplasticity [55, 78, 34], we describe the plastic-like distortions by invoking the Bilby-Kröner-Lee (BKL) decomposition of the deformation gradient tensor, and rephrasing it in a scale-dependent fashion. We remark that, at each of the medium's characteristic scales, a tensor of plastic distortions is introduced, which accounts for the fact that the structural variations of the medium cannot be expressed, in general, in terms of compatible deformations. Our study is conducted within a purely mechanical framework and under the assumption of negligible inertial forces. These hypotheses imply that the model equations reduce to a set comprising a scale-dependent, quasi-static law of balance of linear momentum and an evolution law for the tensor of plastic-like distortions. The latter one is assumed to obey a phenomenological flow rule driven by stress.

The manuscript is organized as follows. In Section 2, we introduce the fundamental notions related to the separation of scales, kinematics, and the Bilby-Kröner-Lee decomposition for the heterogeneous material. Therein, the kinematics of the considered medium is discussed, which has to account for the different length-scales characterizing the heterogeneities and results into the definition of a scale-dependent deformation gradient tensor. In Section 3, the problem to be solved is formulated, and in Section 4, the two-scales asymptotic homogenization technique is applied to obtain the local and the homogenized sub-problems. In Section 5, we prescribe a constitutive equation for the response of the material and, independently, an evolution equation for the tensor of plastic-like distortions. In that respect, the local and homogenized problems derived in Section 4 are formulated by considering the De Saint-Venant strain energy density and we demonstrate the relationship between our new model and the classical ones. In Section 6 we outline a computational scheme to solve the resulting up-scaled model and, in Section 7, we address the numerical results of our simulations. Finally, some concluding remarks on the ongoing work, along with suggestions for future research, are summarized in Section 8. We highlight the novelty of our approach, and we explain how it may contribute to the understanding of the mechanics of heterogeneous media with evolving micro-structure.

2. Theoretical background

2.1. Separation of scales

The homogenization of a highly heterogeneous medium is only possible when the characteristic length of the the local structure (ℓ_0) and the characteristic length of the material, or of the phenomenon, of interest (L_0) are well separated. This condition of separation of scales can be expressed as

$$\varepsilon_0 := \frac{\ell_0}{L_0} \ll 1. \tag{1}$$

There may exist more than two coexisting scales and, if they are well separated from each other, a homogenization approach is possible. In this case, we then move from the smallest scale to the largest one by homogenization [1, 8, 51, 82, 69].

Condition (1) is taken as a base assumption for all homogenization processes. The two characteristic length scales ℓ_0 and L_0 introduce two dimensionless spatial variables in the reference configuration, $\tilde{Y} = X/\ell_0$ and $\tilde{X} = X/L_0$, where X is said to be the *physical spatial variable*, whereas $\tilde{Y}$

and $\tilde{X}$ represent the microscopic and the macroscopic non-dimensional spatial variables, respectively. By using (1), $\tilde{Y}$ and $\tilde{X}$ can be related through the expression

$$\tilde{Y} = \varepsilon_0^{-1} \tilde{X}. \tag{2}$$

Given a field Φ defined over the region of interest of the heterogeneous medium, the separation of scales allows to rephrase the space dependence of Φ as $\Phi(X) = \check{\Phi}(\tilde{X}(X), \tilde{Y}(X))$, and the spatial derivative of Φ takes thus the form

$$\mathrm{Grad}_X \Phi = L_0^{-1} \left(\mathrm{Grad}_{\tilde{X}} \check{\Phi} + \varepsilon_0^{-1} \mathrm{Grad}_{\tilde{Y}} \check{\Phi} \right). \tag{3}$$

By following this approach, all equations should be written in non-dimensional form. In the literature, the switch to the auxiliary variables $\tilde{X}$ and $\tilde{Y}$ is often omitted. However, as shown for example in [4], both paths are equivalent, provided that the dimensional formulation of the problem consistently accounts for any asymptotic behavior of the involved fields and parameters (see e.g. [62] and the discussion therein concerning problems where such a behavior is actually deduced via a non-dimensional analysis). By exploiting this result, in what follows, our analysis is carried out directly in a system of physical variables X and Y. Moreover, by adopting the approach usually followed in asymptotic multiscale analysis, we assume that each field and each material property characterizing the considered medium are functions of both X and Y, with $Y = \varepsilon_0^{-1} X$. Roughly speaking, the dependence on X captures the behavior of a given physical quantity over the largest length-scale, while the dependence on Y captures the behavior over the smallest one. We express this property by introducing the notation $\Phi^\varepsilon(X) = \Phi(X, \varepsilon_0^{-1} X) = \Phi(X, Y)$ [66]. Moreover, for a fixed X, we assume that $\Phi(X, Y)$ is periodic with respect to Y.

In the classical theory of two-scale asymptotic homogenization [5, 8, 14], the small scaling dimensionless parameter ε_0 is constant. However, in the case of a composite material subjected to deformation and change of internal structure (as is the case, for instance, when plastic-like distortions occur), the characteristic macroscopic and microscopic lengths, which refer to the body and to its heterogeneities, respectively, depend on X and t, and should thus be denoted by $\ell(X,t)$ and $L(X,t)$. Therefore, the corresponding scaling parameter, obtained as the ratio $\varepsilon(X,t) = \ell(X,t)/L(X,t)$, is also a function of X and t, which need not be equal to ε_0 in general. This variability notwithstanding, if $\varepsilon(X,t)$ is bounded from above for all X and for all t, and if the upper bound is much smaller than unity, we can indicate such upper bound with ε, and use this constant as a scaling parameter for our asymptotic analysis.

2.2. Kinematics

Let us denote by $\mathcal{B}^\varepsilon$ a continuum body with periodic microstructure, and by $\mathcal{S}$ the three-dimensional Euclidean space. Furthermore, we denote by $\mathcal{B}_0^\varepsilon$ the reference, unloaded configuration of $\mathcal{B}^\varepsilon$, in which the body's periodic micro-structure is reproduced. Now, let us assume that $\chi^\varepsilon : \mathcal{B}_0^\varepsilon \times \mathcal{T} \to \mathcal{S}$ describes the motion of the heterogeneous body, where $\mathcal{T} = [t_0, t_f[$ is an interval of time. Then, the region occupied by the body at time $t \in \mathcal{T}$ is $\mathcal{B}_t^\varepsilon := \chi^\varepsilon(\mathcal{B}_0^\varepsilon, t) \subset \mathcal{S}$ and is said to be its current configuration. Each point $x \in \mathcal{B}_t^\varepsilon$ is such that $x = \chi^\varepsilon(X,t)$, with $X \in \mathcal{B}_0^\varepsilon$ being the point's reference placement. The deformation from $\mathcal{B}_0^\varepsilon$ to $\mathcal{B}_t^\varepsilon$ is characterized by the deformation gradient, $\boldsymbol{F}^\varepsilon(X,t)$, which is defined as $\boldsymbol{F}^\varepsilon(X,t) = T\chi^\varepsilon(X,t)$ [53], with $T\chi^\varepsilon$ being the tangent map of the motion χ^ε, defined from the tangent space $T_X\mathcal{B}_0^\varepsilon$ into $T_x\mathcal{S}$. In the sequel, however, since our focus is on Homogenization Theory, we find it convenient to use the less formal definition

$$\boldsymbol{F}^\varepsilon = \boldsymbol{I} + \mathrm{Grad}\boldsymbol{u}^\varepsilon, \tag{4}$$

where $\boldsymbol{I}$ is the second-order identity tensor and $\mathrm{Grad}\boldsymbol{u}^\varepsilon$ denotes the gradient operator of the displacement $\boldsymbol{u}^\varepsilon$. The condition $J^\varepsilon = \det\boldsymbol{F}^\varepsilon > 0$ must be satisfied in order for χ^ε to be admissible. The symmetric, positive definite, second-order tensor $\boldsymbol{C}^\varepsilon = (\boldsymbol{F}^\varepsilon)^T\boldsymbol{F}^\varepsilon$ is the right Cauchy-Green deformation tensor induced by $\boldsymbol{F}^\varepsilon$. For our purposes, we partition $\mathcal{B}_0^\varepsilon$ into two sub-domains $\mathcal{B}_0^1$ and $\mathcal{B}_0^2$, such that $\bar{\mathcal{B}}_0^1 \cup \bar{\mathcal{B}}_0^2 = \bar{\mathcal{B}}_0^\varepsilon$ and $\bar{\mathcal{B}}_0^1 \cap \mathcal{B}_0^2 = \mathcal{B}_0^1 \cap \bar{\mathcal{B}}_0^2 = \emptyset$, where the bar over a set denotes its closure. We let Γ_0^ε stand for the interface between $\mathcal{B}_0^1$ and $\mathcal{B}_0^2$. Particularly, $\mathcal{B}_0^1$ denotes the matrix of $\mathcal{B}^\varepsilon$ (also referred to as *host phase*) and $\mathcal{B}_0^2$ a collection of N disjoint inclusions. The periodic cell in the reference configuration is denoted by $\mathcal{Y}_0$. The portion of matrix contained in $\mathcal{Y}_0$ is indicated by $\mathcal{Y}_0^1$, while $\mathcal{Y}_0^2$ is the inclusion in $\mathcal{Y}_0$. In each cell, $\mathcal{Y}_0^1$ and $\mathcal{Y}_0^2$ are such that $\bar{\mathcal{Y}}_0^1 \cup \bar{\mathcal{Y}}_0^2 = \bar{\mathcal{Y}}_0$ and $\bar{\mathcal{Y}}_0^1 \cap \mathcal{Y}_0^2 = \mathcal{Y}_0^1 \cap \bar{\mathcal{Y}}_0^2 = \emptyset$. The symbol Γ_0 indicates the interface between $\mathcal{Y}_0^1$ and $\mathcal{Y}_0^2$. In the present work, we assume that the periodicity of the body's micro-structure is preserved even though the body evolves by both changing its shape and varying its internal structure. In general, however, this is not the case. Clearly, our hypothesis is unrealistic in several circumstances, but it might be helpful to describe those situations in which the breaking of the material symmetries occurs at a scale different from those of interest, as is the case, for instance, when the plastic distortions occur in a tissue with evolving material properties [49], that are not directly related to the change of the tissue's micro-geometry. On the other hand, for nonperiodic media, the macro model is still valid when one assumes local boundedness. In that case, the coefficients are simply to be retrieved experimentally, as the "cell" problem is no longer to be computed on the cell but on the whole micro domain, which would be more complex than the original problem.

Moreover, we define $\chi_1^\varepsilon := \chi^\varepsilon|_{\mathcal{B}_0^1} : \mathcal{B}_0^1 \times \mathcal{T} \to \mathcal{S}$ such that $\mathcal{B}_t^1 := \chi_1^\varepsilon(\mathcal{B}_0^1, t)$ denotes the host phase at the current configuration and $\chi_2^\varepsilon := \chi^\varepsilon|_{\mathcal{B}_0^2} : \mathcal{B}_0^2 \times \mathcal{T} \to \mathcal{S}$, with $\mathcal{B}_t^2 := \chi_2^\varepsilon(\mathcal{B}_0^2, t)$ denoting the inclusions. Specifically, we enforce the condition $\bar{\mathcal{B}}_t^1 \cup \bar{\mathcal{B}}_t^2 = \bar{\mathcal{B}}_t^\varepsilon$, with $\bar{\mathcal{B}}_t^1 \cap \mathcal{B}_t^2 = \mathcal{B}_t^1 \cap \bar{\mathcal{B}}_t^2 = \emptyset$, and denote by Γ_t^ε the interface between $\mathcal{B}_t^1$ and $\mathcal{B}_t^2$. In addition, we let $\mathcal{Y}_t$ indicate the periodic cell in the current configuration, with $\bar{\mathcal{Y}}_t^1 \cup \bar{\mathcal{Y}}_t^2 = \bar{\mathcal{Y}}_t$, $\bar{\mathcal{Y}}_t^1 \cap \mathcal{Y}_t^2 = \mathcal{Y}_t^1 \cap \bar{\mathcal{Y}}_t^2 = \emptyset$, and with Γ_t being the interface between $\mathcal{Y}_t^1$ and $\mathcal{Y}_t^2$ (see Fig. 1). We emphasize that $\mathcal{Y}_t^1$ is the portion of matrix and $\mathcal{Y}_t^2$ is the inclusion in $\mathcal{Y}_t$. We note that inside a single cell it can be present also a collection of inclusions and, in such a case, we should consider multiple interface conditions [60].

2.3. Multiplicative decomposition

When the body $\mathcal{B}^\varepsilon$ is subjected to a system of external loads, the change of its shape could be accompanied by a rearrangement of its intrinsic structure. This process is generally inelastic and may not be described just in terms of deformation. Moreover, when mechanical agencies are removed, the body is generally unable to recover the unloaded configuration $\mathcal{B}_0^\varepsilon$, and may occupy a configuration characterized by the presence of residual stresses and strains. To bring the body into a fully relaxed state, an ideal tearing process has to be introduced [55]. More specifically, for each material point $X \in \mathcal{B}^\varepsilon$, we individuate a small neighborhood of X, referred to as *body element*, we ideally cut it out from the body, and we let it relax until it reaches a stress-free state. Such state is the *ground state* of the relaxed body element and is called *natural state*. This concept, originally used in the theory of elasto-plasticity (see [50, 55]), has been used in the biomechanical context by various authors like, for instance, [23, 76, 30, 26, 27, 42, 44, 18, 55, 34, 19]. Before going further with the use of the BKL decomposition, we mention that, in the literature, there exist other approaches to the issue of residual stresses in biological tissues, which call neither for the multiplicative decomposition of the deformation gradient tensor, nor for the introduction of an "intermediate, relaxed configuration". One recent publication adhering to this philosophy is for example [13], in which the authors warn that the intermediate configuration may *"not exist in physical reality and must be postulated a priori"*. Although we are aware of the fact that a framework based on the BKL-decomposition may lead in some cases to assume unrealistic results —as any other framework would do—, we prefer here to adhere to the BKL approach for consistency with previous works of ours.

By performing the ideal process described above for all the body points, a collection of relaxed body pieces is obtained, in which each piece finds itself in its natural state. We denote such collection by $\mathcal{B}^{\varepsilon}_{\nu}$. In the language of continuum mechanics, these physical considerations lead to the BKL decomposition [55, 34]. Although summarizing these theoretical results is useful for sake of completeness, the consequences of the BKL decomposition are well-known, as it is one the pillars of Elastoplasticity. For this reason, we do not fuss over its theoretical justification, and we highlight, rather, the fact that one of the purposes of this work is to investigate the use of a scale-dependent BKL decomposition. In detail, by referring to Figure 1, we invoke a multiplicative decomposition of the deformation gradient $\boldsymbol{F}^{\varepsilon}$ that is parameterized by the scaling ratio ε, i.e.,

$$\boldsymbol{F}^{\varepsilon} = \boldsymbol{F}^{\varepsilon}_{\mathrm{e}} \boldsymbol{F}^{\varepsilon}_{\mathrm{p}}, \tag{5}$$

where the tensors $\boldsymbol{F}^{\varepsilon}_{\mathrm{e}}$ and $\boldsymbol{F}^{\varepsilon}_{\mathrm{p}}$ describe, respectively, the elastic and the inelastic distortions contributing to $\boldsymbol{F}^{\varepsilon}$ Along with (5), we also define the determinants $J^{\varepsilon}_{\mathrm{e}} = \det()F^{\varepsilon}_{\mathrm{e}}$ and $J^{\varepsilon}_{\mathrm{p}} = \det()F^{\varepsilon}_{\mathrm{p}}$, which are both strictly positive. Consistently with the notation introduced above, it holds true that $\boldsymbol{F}^{\varepsilon}_{\mathrm{e}}(X) = \boldsymbol{F}_{\mathrm{e}}(X, Y)$, $\boldsymbol{F}^{\varepsilon}_{\mathrm{p}}(X) = \boldsymbol{F}_{\mathrm{p}}(X, Y)$, and $\boldsymbol{F}^{\varepsilon}(X) = \boldsymbol{F}(X, Y)$ as well as $J^{\varepsilon}_{\mathrm{e}}(X) = J_{\mathrm{e}}(X, Y)$ and $J^{\varepsilon}_{\mathrm{p}}(X) = J_{\mathrm{p}}(X, Y)$.

In this work, we focus on remodeling, i.e., plastic-like distortions that occur to modify the internal structure of $\mathcal{B}^{\varepsilon}$. Although this phenomenon is not visible, it could lead to the alteration of the mechanical properties of $\mathcal{B}^{\varepsilon}$.

3. Formulation of the problem

We consider a composite material comprising two solid constituents, whose point-wise constitutive response is hyperelastic. Therefore, to model its mechanical behavior, we introduce the scale-dependent strain energy function,

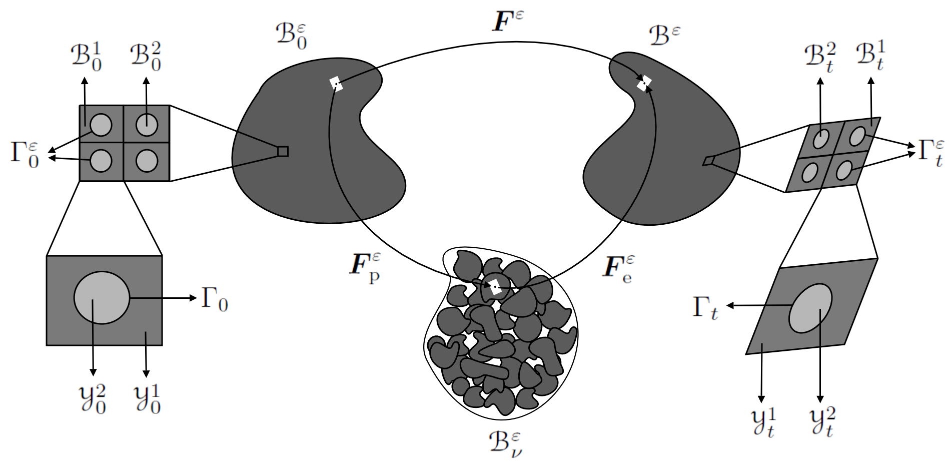

Figure 1: Schematic of a composite material with periodic internal micro-structure and subjected to inelastic remodeling distortions. From left to right: Magnification of an excerpt of material and description of its nested, periodic micro-structure. Change of shape of the body from the reference to the current configuration, and definition of the conglomerate of relaxed body pieces, each in its natural state. Magnification of an excerpt of material, taken from the body's current configuration, and description of its deformed, and remodeled, micro-structure.

defined per unit volume of the natural state,

$$\check{\psi}_\nu(X,t) = \psi_\nu^\varepsilon(\boldsymbol{F}_\mathrm{e}^\varepsilon(X,t), i^\varepsilon(X,t)) = \psi_\nu(\boldsymbol{F}_\mathrm{e}(X,Y,t), i(X,Y,t)), \tag{6}$$

where i is defined by the expression $i(X,Y,t) = (X,Y)$, i.e., i extracts the spatial pair (X,Y) from the triplet (X,Y,t). From (6) we can derive the first Piola-Kirchoff stress tensor,

$$\boldsymbol{T}^\varepsilon = J_\mathrm{p}^\varepsilon \frac{\partial \psi_\nu^\varepsilon}{\partial \boldsymbol{F}_\mathrm{e}^\varepsilon} \left(\boldsymbol{F}_\mathrm{p}^\varepsilon\right)^{-T}, \tag{7}$$

where $J_\mathrm{p}^\varepsilon = \det \boldsymbol{F}_\mathrm{p}^\varepsilon$. In particular, if we neglect body forces and inertial terms, the balance of linear momentum reads,

$$\begin{cases} \mathrm{Div}\, \boldsymbol{T}^\varepsilon = \boldsymbol{0}, & \text{in } \mathcal{B}_0^\varepsilon \setminus \Gamma_0^\varepsilon \times \mathcal{T}, \\ \boldsymbol{T}^\varepsilon \cdot \boldsymbol{N} = \bar{\boldsymbol{T}}, & \text{on } \partial_T \mathcal{B}_0^\varepsilon \times \mathcal{T}, \\ \boldsymbol{u}^\varepsilon = \bar{\boldsymbol{u}}, & \text{on } \partial_u \mathcal{B}_0^\varepsilon \times \mathcal{T}, \end{cases} \tag{8}$$

where $\bar{\boldsymbol{T}}$ and $\bar{\boldsymbol{u}}$ are, respectively, the prescribed traction and displacement on the boundary $\partial\mathcal{B}_0^\varepsilon = \partial_T\mathcal{B}_0^\varepsilon \cup \partial_u\mathcal{B}_0^\varepsilon$ with $\overline{\partial_T\mathcal{B}_0^\varepsilon} \cap \partial_u\mathcal{B}_0^\varepsilon = \partial_T\mathcal{B}_0^\varepsilon \cap \overline{\partial_u\mathcal{B}_0^\varepsilon} = \emptyset$

and $\boldsymbol{N}$ is the outward unit vector normal to the surface $\partial\mathcal{B}_0^\varepsilon$. Continuity conditions for displacement and traction are imposed,

$$[\![\boldsymbol{u}^\varepsilon]\!] = \boldsymbol{0} \quad \text{and} \quad [\![\boldsymbol{T}^\varepsilon \cdot \boldsymbol{N}_{\mathcal{Y}}]\!] = \boldsymbol{0}, \quad \text{on } \Gamma_0 \times \mathcal{T}, \tag{9}$$

where $[\![\bullet]\!]$ denotes the jump across the interface between the two constituents and $\boldsymbol{N}_{\mathcal{Y}}$ defines the unit outward normal to Γ_0. Moreover, problem (8) must be supplemented with an appropriate evolution law for $\boldsymbol{F}_{\mathrm{p}}^\varepsilon$. It is worth mentioning that the homogenization process can be performed regardless of the particular choice of *external* boundary conditions (Dirichlet-Neumann in this case). This means that the formulation presented in this work is potentially applicable also to other external boundary conditions, such as e.g. those of Robin-type. This is due to the fact that, as pointed out in [69], also in the present study the homogenization is applied in regions sufficiently far away from the outer boundary of the considered medium. For problems in which it is necessary to homogenize also close to the outer heterogeneous boundaries, we refer to [8, 57, 46].

Remark 1. *In the present work, we impose conditions* (9) *for displacements and tractions just to exemplify the homogenization technique applied to heterogeneous media with evolving microstructure. In other words, we assume that the contact interface between the constituents is ideal. This means that the displacements are congruent, and thus continuous, and that linear momentum is conserved across the interface, which in our context implies the continuity of the tractions. However, the hypothesis of the ideal interface can be relaxed in some biological situations. For instance, in cancerous tissues, there exist cross-links between normal and malignant cells, whose density and strength determine a spring constant that relates the normal stresses on each cell surface, thereby making it non-ideal [47, 37]. Another example of non-ideal interface is the periodontal ligament, which represents the thin layer between the cementum of the tooth to the adjacent alveolar bone [28]. In the context of composite materials, when non-ideal interfaces are accounted for, the interface conditions are suitably reformulated [38, 39, 7, 6]. In particular, the asymptotic homogenization technique has been applied for linear elastic periodic fiber reinforced composites with imperfect contact between matrix and fibers (see e.g. [36]).*

4. Asymptotic homogenization of the balance of linear momentum

A formal two-scale asymptotic expansion is performed for the displacement $\boldsymbol{u}^\varepsilon$, which thus reads

$$\boldsymbol{u}^\varepsilon(X,t) = \boldsymbol{u}^{(0)}(X,t) + \sum_{k=1}^{+\infty} \boldsymbol{u}^{(k)}(X,Y,t)\varepsilon^k, \tag{10}$$

where, for all $k \geq 1$, $\boldsymbol{u}^{(k)}$ is periodic with respect to Y. Following [68] we consider the leading order term of the expansion (10) to be independent of the fast variable Y. From formula (4), the expansion (10), and taking into account the property of scale separation, it follows that the deformation gradient tensor can be written as

$$\boldsymbol{F}^\varepsilon(X,t) = \sum_{k=0}^{+\infty} \boldsymbol{F}^{(k)}(X,Y,t)\varepsilon^k, \tag{11}$$

with the notation

$$\boldsymbol{F}^{(0)} := \boldsymbol{I} + \mathrm{Grad}_X \boldsymbol{u}^{(0)} + \mathrm{Grad}_Y \boldsymbol{u}^{(1)}, \tag{12a}$$

$$\boldsymbol{F}^{(k)} := \mathrm{Grad}_X \boldsymbol{u}^{(k)} + \mathrm{Grad}_Y \boldsymbol{u}^{(k+1)}, \quad \forall\, k \geq 1, \tag{12b}$$

where Grad_X and Grad_Y are the gradient operators with respect to X and Y, respectively. Now, the following two-scale asymptotic expansion is proposed for the first Piola-Kirchhoff stress tensor $\boldsymbol{T}^\varepsilon$,

$$\boldsymbol{T}^\varepsilon(X,t) = \sum_{k=0}^{+\infty} \boldsymbol{T}^{(k)}(X,Y,t)\varepsilon^k, \tag{13}$$

where the fields $\boldsymbol{T}^{(k)}$ are periodic with respect to Y. By substituting the power series representation (13) into (8), using the scale separation condition, and multiplying the result by ε, the following multi-scale system is obtained

$$\mathrm{Div}\, \boldsymbol{T}^\varepsilon = \sum_{k=0}^{+\infty} \mathfrak{D}^{(k)}\varepsilon^k = \boldsymbol{0}, \tag{14}$$

with

$$\mathfrak{D}^{(0)} := \mathrm{Div}_Y \boldsymbol{T}^{(0)}, \tag{15a}$$

$$\mathfrak{D}^{(k)} := \mathrm{Div}_X \boldsymbol{T}^{(k-1)} + \mathrm{Div}_Y \boldsymbol{T}^{(k)}, \quad \forall\, k \geq 1. \tag{15b}$$

We require that the equilibrium equation (14) is satisfied at every ε, which amounts to impose the conditions

$$\mathrm{Div}_Y \boldsymbol{T}^{(0)} = \mathbf{0}, \tag{16a}$$

$$\mathrm{Div}_X \boldsymbol{T}^{(k-1)} + \mathrm{Div}_Y \boldsymbol{T}^{(k)} = \mathbf{0}, \quad \forall\, k \geq 1. \tag{16b}$$

At this point we introduce the average operator over the microscopic cell, i.e.

$$\langle \bullet \rangle = \frac{1}{|\mathcal{Y}_t|} \int_{\mathcal{Y}_t} \bullet \, \mathrm{d}Y, \tag{17}$$

where $|\mathcal{Y}_t|$ represents the volume of the periodic cell $\mathcal{Y}_t$ at time t. Indeed, because of the deformations and distortions to which the microscopic, reference periodic cell is subjected, $\mathcal{Y}_t$ is different at every time instant. Averaging (16b) over the microscopic cell yields, for $k = 1$,

$$\langle \mathrm{Div}_X \boldsymbol{T}^{(0)} \rangle + \frac{1}{|\mathcal{Y}_t|} \int_{\partial \mathcal{Y}_t} \boldsymbol{T}^{(1)} \cdot \boldsymbol{N} \mathrm{d}Y = \mathbf{0}, \tag{18}$$

where, on the left-hand side, we have applied the divergence theorem. Since the contributions on the periodic cell boundary $\partial \mathcal{Y}_t$ cancel due to the Y-periodicity, the integral over $\mathcal{Y}_t$ is equal to zero, and (18) becomes

$$\langle \mathrm{Div}_X \boldsymbol{T}^{(0)} \rangle = \mathbf{0}. \tag{19}$$

Here, we restrict our analysis to the particular case in which the periodic cell can be uniquely chosen independently of X, which implies that the integration over $\mathcal{Y}_t$ and the computation of the divergence commute. This assumption is also referred to as *macroscopic uniformity*, see also [9, 40, 59] for examples dealing with non-macroscopically uniform media in the context of poroelasticity and diffusion. Therefore, Equation (19) can be recast as

$$\mathrm{Div}_X \langle \boldsymbol{T}^{(0)} \rangle = \mathbf{0}. \tag{20}$$

Equations (16a) and (20) represent, respectively, the local and the homogenized equation associated with the original one, stated in (8). Both equations still need to be supplemented with the corresponding interface, boundary, and initial conditions. Note that, although both problems feature no time derivative, initial conditions are required because $\boldsymbol{T}^{(0)}$ depends on the variable $\boldsymbol{F}_{\rm p}^{(0)}$, which satisfies an evolution equation in time.

We remark that the leading term $\boldsymbol{T}^{(0)} = \boldsymbol{T}^{(0)}(X, Y, t)$ of the multi-scale expansion (13) is the unknown, both in (16a) and in (20). To identify $\boldsymbol{T}^{(0)}$, we propose here to expand $\boldsymbol{F}_{\rm p}^{\varepsilon}$ and ψ_{ν}^{ε} as

$$\boldsymbol{F}_{\rm p}^{\varepsilon}(X,t) = \sum_{k=0}^{+\infty} \boldsymbol{F}_{\rm p}^{(k)}(X,Y,t)\varepsilon^k, \tag{21a}$$

$$\psi_{\nu}^{\varepsilon}(X,t) = \sum_{k=0}^{+\infty} \psi_{\nu}^{(k)}(\boldsymbol{F}_{\rm e}(X,Y,t),X,Y)\varepsilon^k, \tag{21b}$$

where $\boldsymbol{F}_{\rm p}^{(k)}$ and $\psi_{\nu}^{(k)}$ are periodic in Y. By using (5), (11) and (21a), we can deduce a series expansion for $\boldsymbol{F}_{\rm e}^{\varepsilon}$ in powers of ε, where the leading order term $\boldsymbol{F}_{\rm e}^{(0)}$ is given by

$$\boldsymbol{F}_{\rm e}^{(0)} = \boldsymbol{F}^{(0)}(\boldsymbol{F}_{\rm p}^{(0)})^{-1}. \tag{22}$$

Following [15] and [68], $\boldsymbol{T}^{(0)}$ is therefore supplied constitutively as

$$\boldsymbol{T}^{(0)} = J_{\rm p}^{(0)} \frac{\partial \psi_{\nu}^{(0)}}{\partial \boldsymbol{F}_{\rm e}^{(0)}} (\boldsymbol{F}_{\rm p}^{(0)})^{-T}, \tag{23}$$

with $\psi_{\nu}^{(0)} = \psi_{\nu}^{(0)}(\boldsymbol{F}_{\rm e}^{(0)}(X,Y,t),X,Y)$ and $J_{\rm p}^{(0)} = \det \boldsymbol{F}_{\rm p}^{(0)}$. To obtain the *cell problem*, equation (14) must be supplemented with the corresponding interface conditions. This is done by substituting the asymptotic expansions of $\boldsymbol{u}^{\varepsilon}$ and of $\boldsymbol{T}^{\varepsilon}$ into the interface conditions $[\![\boldsymbol{u}^{\varepsilon}]\!] = \boldsymbol{0}$ and $[\![\boldsymbol{T}^{\varepsilon} \cdot \boldsymbol{N}_{\mathcal{Y}}]\!] = \boldsymbol{0}$. Both conditions are satisfied at any order of ε. At the order ε^0, we simply obtain $[\![\boldsymbol{T}^{(0)} \cdot \boldsymbol{N}_{\mathcal{Y}}]\!] = \boldsymbol{0}$ for the stresses, and that the condition $[\![\boldsymbol{u}^{(0)}]\!] = \boldsymbol{0}$ is trivially satisfied, because $\boldsymbol{u}^{(0)}$ depends solely on X and t. Thus, the interface condition on the displacements is written only for $\boldsymbol{u}^{(1)}$ and reads, $[\![\boldsymbol{u}^{(1)}]\!] = \boldsymbol{0}$. By summarizing these results, the cell problem at zero order of the epsilon parameter can be stated as

$$\begin{cases} \mathrm{Div}_Y \boldsymbol{T}^{(0)} = \boldsymbol{0}, & \text{in } \mathcal{Y}_0 \setminus \Gamma_0 \times \mathcal{T}, \\ [\![\boldsymbol{u}^{(1)}]\!] = \boldsymbol{0}, & \text{on } \Gamma_0 \times \mathcal{T}, \\ [\![\boldsymbol{T}^{(0)} \cdot \boldsymbol{N}_{\mathcal{Y}}]\!] = \boldsymbol{0}, & \text{on } \Gamma_0 \times \mathcal{T}. \end{cases} \tag{24}$$

Together with the cell problem, we also need to formulate the macro-scopic homogenized problem. To this end, we take equation (20) and complete it with a set of boundary conditions. This is done by substituting the asymptotic expansions of $\boldsymbol{T}^{\varepsilon}$ and $\boldsymbol{u}^{\varepsilon}$ into the boundary conditions $\boldsymbol{T}^{\varepsilon} \cdot \boldsymbol{N} = \bar{\boldsymbol{T}}$ and $\boldsymbol{u}^{\varepsilon} = \bar{\boldsymbol{u}}$, respectively. Thus, equating the coefficients at order ε^0, and averaging the results over the unit cell, we find the *homogenized problem*,

$$\begin{cases} \mathrm{Div}_X \langle \boldsymbol{T}^{(0)} \rangle = \boldsymbol{0}, & \text{in } \mathcal{B}_h \times \mathcal{T}, \\ \langle \boldsymbol{T}^{(0)} \rangle \cdot \boldsymbol{N} = \bar{\boldsymbol{T}}, & \text{on } \partial_T \mathcal{B}_h \times \mathcal{T}, \\ \boldsymbol{u}^{(0)} = \bar{\boldsymbol{u}}, & \text{on } \partial_u \mathcal{B}_h \times \mathcal{T}, \end{cases} \tag{25}$$

where $\mathcal{B}_h$ denotes the homogeneous macro-scale domain in which the homogenized equations are defined.

The problem (25) has to be solved along with a homogenized evolution equation for $\boldsymbol{F}_{\mathrm{p}}^{(0)}$ and the initial condition associated with it. In addition, we remark that, according to (25), the boundary tractions acting on $\partial_T \mathcal{B}_h$ are balanced *only* by the normal component of the average of the leading order stress, $\boldsymbol{T}^{(0)}$, and *only* the leading order displacement, $\boldsymbol{u}^{(0)}$, has to be equal to the displacement $\bar{\boldsymbol{u}}$, imposed on $\partial_u \mathcal{B}_h$.

Remark 2. *In the medical scientific literature, there exist studies that identify the existence of anatomical boundary layers interposed between the brain surface and tumors (see e.g. [72]). Here we do not address boundary layer phenomena, which are usually neglected in the asymptotic homogenization literature. The homogenization process described in this work is fine for regions far enough away from the boundary so that its effect is not felt because, close to the boundaries, the material will not behave as an effective material with homogenized coefficients. To properly account for boundary effects, the so-called boundary-layer technique could be used [8, 57].*

5. Constitutive framework and evolution law

In this section, we prescribe a constitutive equation for the response of the material and, independently, an evolution equation for the tensor of plastic-like distortions.

5.1. Constitutive law

In the following, we formulate the local and homogenized problems for a specific constitutive law. In general, this process can be rather cumbersome for complicated strain energy densities, and it becomes even more involved when plastic-like distortions are accounted for. To reduce complexity, we choose a very simple constitutive law for ψ_ν^ε, such as the De Saint-Venant strain energy density,

$$\psi_\nu^\varepsilon = \frac{1}{2}\boldsymbol{E}_{\mathrm{e}}^\varepsilon : \mathscr{C}^\varepsilon : \boldsymbol{E}_{\mathrm{e}}^\varepsilon, \tag{26}$$

where $\boldsymbol{E}_{\mathrm{e}}^\varepsilon = \frac{1}{2}\left((\boldsymbol{F}_{\mathrm{e}}^\varepsilon)^T \boldsymbol{F}_{\mathrm{e}}^\varepsilon - \boldsymbol{I}\right)$ is the elastic Green-Lagrange strain tensor and $\mathscr{C}^\varepsilon(X) = \mathscr{C}(X, Y)$ is the positive definite fourth-order elasticity tensor, which satisfies both major and minor symmetries, i.e. $\mathscr{C}_{ijkl} = \mathscr{C}_{jikl} = \mathscr{C}_{ijlk} = \mathscr{C}_{klij}$. Particularly, we consider that the constituents of the heterogeneous material are isotropic, and thus

$$\mathscr{C}^\varepsilon = 3\kappa^\varepsilon \mathscr{K} + 2\mu^\varepsilon \mathscr{M}, \tag{27}$$

where $\kappa^\varepsilon(X) = \kappa(X, Y)$ is the bulk modulus, $\mu^\varepsilon(X) = \mu(X, Y)$ is the shear modulus, and the fourth-order tensors $\mathscr{K} = \frac{1}{3}(\boldsymbol{I} \otimes \boldsymbol{I})$ and $\mathscr{M} = \mathscr{I} - \mathscr{K}$ extract the spherical and the deviatoric part, respectively, of a symmetric second-order tensor $\boldsymbol{A}$, i.e., $\mathscr{K} : \boldsymbol{A} = \frac{1}{3}\mathrm{tr}(\boldsymbol{A})\boldsymbol{I}$ and $\mathscr{M} : \boldsymbol{A} = \boldsymbol{A} - \frac{1}{3}\mathrm{tr}(\boldsymbol{A})\boldsymbol{I} := \mathrm{dev}(\boldsymbol{A})$ [84, 85]. We remark that the fourth-order identity tensor $\mathscr{I}$ is the identity operator over the linear subspace of symmetric second-order tensors. Indeed, for every $\boldsymbol{A}$ such that $\boldsymbol{A} = \boldsymbol{A}^T$, it holds that $\mathscr{I} : \boldsymbol{A} = \boldsymbol{A}$. In terms of $\boldsymbol{I}$, an explicit expression of $\mathscr{I}$ is given by $\mathscr{I} = \frac{1}{2}\left[\boldsymbol{I} \underline{\otimes} \boldsymbol{I} + \boldsymbol{I} \overline{\otimes} \boldsymbol{I}\right]$ (in components: $\mathscr{I}_{ijkl} = \frac{1}{2}\left[I_{ik}I_{jl} + I_{il}I_{jk}\right]$ [17]).

We can identify the leading order term in the expansion of the constitutive law (26), which reads

$$\psi_\nu^{(0)} = \frac{1}{2}\boldsymbol{E}_{\mathrm{e}}^{(0)} : \mathscr{C} : \boldsymbol{E}_{\mathrm{e}}^{(0)}, \tag{28}$$

with $\boldsymbol{E}_{\mathrm{e}}^{(0)} = \frac{1}{2}\left((\boldsymbol{F}_{\mathrm{e}}^{(0)})^T \boldsymbol{F}_{\mathrm{e}}^{(0)} - \boldsymbol{I}\right)$. We recall that, although the expression of $\psi_\nu^{(0)}$ in (28) depends only on $\boldsymbol{E}_{\mathrm{e}}^{(0)}$, the material coefficient $\mathscr{C}$ is still a two-scale function and should be thus interpreted as $\mathscr{C}(X, Y)$. As a consequence, $\psi_\nu^{(0)}$ is not homogenized yet.

By taking into account the major and minor symmetries of $\mathscr{C}$, we obtain

$$\boldsymbol{S}_\nu^{(0)} = \frac{\partial \psi_\nu^{(0)}}{\partial \boldsymbol{E}_{\mathrm{e}}^{(0)}} = \mathscr{C} : \boldsymbol{E}_{\mathrm{e}}^{(0)} = \lambda \mathrm{tr}(\boldsymbol{E}_{\mathrm{e}}^{(0)})\boldsymbol{I} + 2\mu \boldsymbol{E}_{\mathrm{e}}^{(0)}, \tag{29}$$

where $\boldsymbol{S}_{\nu}^{(0)}$ is the leading order term of the second Piola-Kirchhoff stress tensor written with respect to the natural state, $\lambda = \kappa - \frac{2}{3}\mu$ is Lamé's constant, and $\boldsymbol{E}_{\mathrm{e}}^{(0)}$ is given by

$$\boldsymbol{E}_{\mathrm{e}}^{(0)} = (\boldsymbol{F}_{\mathrm{p}}^{(0)})^{-T}\left(\boldsymbol{E}^{(0)} - \boldsymbol{E}_{\mathrm{p}}^{(0)}\right)(\boldsymbol{F}_{\mathrm{p}}^{(0)})^{-1}, \tag{30}$$

with $\boldsymbol{E}^{(0)} = \frac{1}{2}\left((\boldsymbol{F}^{(0)})^T\boldsymbol{F}^{(0)} - \boldsymbol{I}\right)$ and $\boldsymbol{E}_{\mathrm{p}}^{(0)} = \frac{1}{2}\left((\boldsymbol{F}_{\mathrm{p}}^{(0)})^T\boldsymbol{F}_{\mathrm{p}}^{(0)} - \boldsymbol{I}\right)$.

By pulling $\boldsymbol{S}_{\nu}^{(0)}$ back to the reference configuration, and recalling that the plastic-like distortions are assumed to be isochoric in our framework, (i.e. $J_{\mathrm{p}}^{\varepsilon} = 1$), we obtain the second Piola-Kirchhoff stress tensor

$$\boldsymbol{S}^{(0)} = \mathscr{C}_{\mathrm{R}} : (\boldsymbol{E}^{(0)} - \boldsymbol{E}_{\mathrm{p}}^{(0)}), \tag{31}$$

where

$$\begin{aligned}\mathscr{C}_{\mathrm{R}} &= (\boldsymbol{F}_{\mathrm{p}}^{(0)})^{-1} \,\underline{\otimes}\, (\boldsymbol{F}_{\mathrm{p}}^{(0)})^{-1} : \mathscr{C} : (\boldsymbol{F}_{\mathrm{p}}^{(0)})^{-T} \,\underline{\otimes}\, (\boldsymbol{F}_{\mathrm{p}}^{(0)})^{-T} \\ &= 3\lambda\mathscr{K}_{\mathrm{p}}^{(0)} + 2\mu\mathscr{I}_{\mathrm{p}}^{(0)},\end{aligned} \tag{32}$$

is the elasticity tensor pulled-back to the reference configuration through $\boldsymbol{F}_{\mathrm{p}}^{(0)}$, and, upon setting $\boldsymbol{B}_{\mathrm{p}}^{(0)} = (\boldsymbol{F}_{\mathrm{p}}^{(0)})^{-1}(\boldsymbol{F}_{\mathrm{p}}^{(0)})^{-T}$, we employed the notation

$$\mathscr{K}_{\mathrm{p}}^{(0)} = \tfrac{1}{3}\boldsymbol{B}_{\mathrm{p}}^{(0)} \otimes \boldsymbol{B}_{\mathrm{p}}^{(0)}, \tag{33a}$$

$$\mathscr{I}_{\mathrm{p}}^{(0)} = \tfrac{1}{2}\left[\boldsymbol{B}_{\mathrm{p}}^{(0)}\underline{\otimes}\boldsymbol{B}_{\mathrm{p}}^{(0)} + \boldsymbol{B}_{\mathrm{p}}^{(0)}\overline{\otimes}\boldsymbol{B}_{\mathrm{p}}^{(0)}\right]. \tag{33b}$$

We remark that $\mathscr{K}_{\mathrm{p}}^{(0)}$ extracts the "volumetric part" of a generic second-order tensor, taken with respect to the inverse plastic metric tensor $\boldsymbol{B}_{\mathrm{p}}^{(0)}$ i.e. for all $\boldsymbol{A} = \boldsymbol{A}^T$, it holds that $\mathscr{K}_{\mathrm{p}}^{(0)} : \boldsymbol{A} = \frac{1}{3}\mathrm{tr}(\boldsymbol{B}_{\mathrm{p}}^{(0)}\boldsymbol{A})\boldsymbol{B}_{\mathrm{p}}^{(0)}$. Furthermore, $\mathscr{I}_{\mathrm{p}}^{(0)}$ transforms $\boldsymbol{A}$ into $\mathscr{I}_{\mathrm{p}}^{(0)} : \boldsymbol{A} = \boldsymbol{B}_{\mathrm{p}}^{(0)}\boldsymbol{A}\boldsymbol{B}_{\mathrm{p}}^{(0)}$ and $\mathscr{M}_{\mathrm{p}}^{(0)} = \mathscr{I}_{\mathrm{p}}^{(0)} - \mathscr{K}_{\mathrm{p}}^{(0)}$ extracts the "deviatoric part" of $\boldsymbol{A}$ with respect to the metric tensor $\boldsymbol{B}_{\mathrm{p}}^{(0)}$, i.e. $\mathscr{M}_{\mathrm{p}}^{(0)} : \boldsymbol{A} = \boldsymbol{B}_{\mathrm{p}}^{(0)}\boldsymbol{A}\boldsymbol{B}_{\mathrm{p}}^{(0)} - \frac{1}{3}\mathrm{tr}(\boldsymbol{B}_{\mathrm{p}}^{(0)}\boldsymbol{A})\boldsymbol{B}_{\mathrm{p}}^{(0)}$. We note that similar results have been obtained in the case of non-linear elasticity in [25].

Next, we notice that $\boldsymbol{F}^{(0)}$ can be written as

$$\boldsymbol{F}^{(0)} = \boldsymbol{I} + \boldsymbol{H}, \tag{34}$$

with $\boldsymbol{H} = \mathrm{Grad}_X\boldsymbol{u}^{(0)} + \mathrm{Grad}_Y\boldsymbol{u}^{(1)}$. Thus, by substituting (34) in $\boldsymbol{E}_{\mathrm{e}}^{(0)}$, the result into (31), and retaining only the terms linear in $\boldsymbol{H}$, $\boldsymbol{S}^{(0)}$ can be linearized as

$$\boldsymbol{S}_{\mathrm{lin}}^{(0)} = \mathscr{C}_{\mathrm{R}} : (\mathrm{sym}\boldsymbol{H} - \boldsymbol{E}_{\mathrm{p}}^{(0)}). \tag{35}$$

We recall now that, at the leading order, the first Piola-Kirchhoff stress tensor reads $\boldsymbol{T}^{(0)} = \boldsymbol{F}^{(0)}\boldsymbol{S}^{(0)}$. Hence, its linearized form is given by

$$\boldsymbol{T}^{(0)}_{\text{lin}} = \mathscr{C}_{\text{R}} : \text{sym}\boldsymbol{H} - (\boldsymbol{I} + \boldsymbol{H})(\mathscr{C}_{\text{R}} : \boldsymbol{E}^{(0)}_{\text{p}}). \tag{36}$$

Looking at the definition of $\mathscr{C}_{\text{R}}$ in (32), it can be noticed that our model resolves at the macro-scale the structural evolution of the considered medium through the dependence of $\mathscr{C}_{\text{R}}$ on $\boldsymbol{F}^{(0)}_{\text{p}}$, which indeed describes the production of material inhomogeneities [21, 22, 23]. Additionally, our model is also capable of simultaneously resolving the material heterogeneities at both the micro- and macro-scale through the dependence of $\mathscr{C}_{\text{R}}$ on X and Y. The latter dependence in fact, keeps track of the variability of the elastic coefficient at both scales.

Because of Equations (33a) and (33b), $\mathscr{C}_{\text{R}}$ possesses the same symmetry properties of $\mathscr{C}$, i.e.

$$(\mathscr{C}_{\text{R}})_{IJKL} = (\mathscr{C}_{\text{R}})_{JIKL} = (\mathscr{C}_{\text{R}})_{IJLK} = (\mathscr{C}_{\text{R}})_{KLIJ}, \tag{37}$$

and therefore, $\boldsymbol{T}^{(0)}_{\text{lin}}$ can be written as

$$\boldsymbol{T}^{(0)}_{\text{lin}} = \mathscr{C}_{\text{R}} : \boldsymbol{H} - (\boldsymbol{I} + \boldsymbol{H})(\mathscr{C}_{\text{R}} : \boldsymbol{E}^{(0)}_{\text{p}}). \tag{38}$$

Local problem. Substituting (38) in the equation of the local problem (24), the linear momentum balance law is rephrased as

$$\text{Div}_Y\big[\mathscr{C}_{\text{R}} : \boldsymbol{H} - (\boldsymbol{I} + \boldsymbol{H})(\mathscr{C}_{\text{R}} : \boldsymbol{E}^{(0)}_{\text{p}})\big] = \boldsymbol{0}, \tag{39}$$

or, equivalently,

$$\begin{aligned}&\text{Div}_Y\big[\mathscr{C}_{\text{R}} : \text{Grad}_Y\boldsymbol{u}^{(1)} - \text{Grad}_Y\boldsymbol{u}^{(1)}(\mathscr{C}_{\text{R}} : \boldsymbol{E}^{(0)}_{\text{p}})\big] = \\ &- \text{Div}_Y\big[\mathscr{C}_{\text{R}} : \text{Grad}_X\boldsymbol{u}^{(0)} - (\boldsymbol{I} + \text{Grad}_X\boldsymbol{u}^{(0)})(\mathscr{C}_{\text{R}} : \boldsymbol{E}^{(0)}_{\text{p}})\big].\end{aligned} \tag{40}$$

In the absence of plastic distortions, i.e., when $\boldsymbol{F}^{\varepsilon}_{\text{p}} = \boldsymbol{I}$, Equation (40) coincides with the equation of the classical cell problem encountered in the homogeneization of linear elasticity, which is known to admit a unique solution, up to a Y-constant function, if the average over the cell of the right-hand-side vanishes identically (in the jargon of Homogenization Theory, this condition is referred to as *solvability condition* or *compatibility condition*) [5]. In our case, since the pulled-back elasticity tensor $\mathscr{C}_{\mathrm{R}}$ is periodic in Y, while $\boldsymbol{u}^{(0)}$ is independent of Y, the solvability condition is satisfied, i.e.,

$$\left\langle \mathrm{Div}_Y \left[\mathscr{C}_{\mathrm{R}} : \mathrm{Grad}_X \boldsymbol{u}^{(0)} - (\boldsymbol{I} + \mathrm{Grad}_X \boldsymbol{u}^{(0)})(\mathscr{C}_{\mathrm{R}} : \boldsymbol{E}_{\mathrm{p}}^{(0)}) \right] \right\rangle = \boldsymbol{0}. \tag{41}$$

Exploiting the linearity of equation (40) in $\boldsymbol{u}^{(1)}$, we make the *ansatz*

$$\boldsymbol{u}^{(1)}(X, Y, t) = \boldsymbol{\xi}(X, Y, t) : \mathrm{Grad}_X \boldsymbol{u}^{(0)}(X, t) + \boldsymbol{\omega}(X, Y, t), \tag{42}$$

where $\boldsymbol{\xi}$ and $\boldsymbol{\omega}$ are a third-order tensor field and a vector field, both periodic in Y.

We now require that $\boldsymbol{\xi}$ and $\boldsymbol{\omega}$ satisfy two independent cell problems. The cell problem for $\boldsymbol{\xi}$ reads

$$\begin{cases} \mathrm{Div}_Y \left[\mathscr{C}_{\mathrm{R}} : T\mathrm{Grad}_Y \boldsymbol{\xi} - T\mathrm{Grad}_Y \boldsymbol{\xi} (\mathscr{C}_{\mathrm{R}} : \boldsymbol{E}_{\mathrm{p}}^{(0)}) \right] & \\ \quad = \mathrm{Div}_Y \left[-\mathscr{C}_{\mathrm{R}} + \boldsymbol{I} \underline{\otimes} (\mathscr{C}_{\mathrm{R}} : \boldsymbol{E}_{\mathrm{p}}^{(0)}) \right], & \text{in } \mathcal{Y}_0 \setminus \Gamma_0 \times \mathcal{T}, \\ [\![\boldsymbol{\xi}]\!] = \boldsymbol{0}, & \text{on } \Gamma_0 \times \mathcal{T}, \\ [\![\left[\mathscr{C}_{\mathrm{R}} : T\mathrm{Grad}_Y \boldsymbol{\xi} - T\mathrm{Grad}_Y \boldsymbol{\xi} (\mathscr{C}_{\mathrm{R}} : \boldsymbol{E}_{\mathrm{p}}^{(0)}) \right. & \\ \quad \left. + \mathscr{C}_{\mathrm{R}} - \boldsymbol{I} \underline{\otimes} (\mathscr{C}_{\mathrm{R}} : \boldsymbol{E}_{\mathrm{p}}^{(0)}) \right] \cdot \boldsymbol{N}_{\mathcal{Y}}]\!] = \boldsymbol{0}, & \text{on } \Gamma_0 \times \mathcal{T}. \end{cases} \tag{43}$$

Before going further, some words of explanation on the notation are necessary. First, we notice that $\mathrm{Grad}_Y \boldsymbol{\xi}$ is a fourth-order tensor function, which admits the representation $\mathrm{Grad}_Y \boldsymbol{\xi} = (\partial \xi_{ABC})/(\partial Y_D) \boldsymbol{e}_A \otimes \boldsymbol{e}_B \otimes \boldsymbol{e}_C \otimes \boldsymbol{e}_D$. Then, $T\mathrm{Grad}_Y \boldsymbol{\xi}$ is a fourth-order tensor function obtained by ordering the indices of $\mathrm{Grad}_Y \boldsymbol{\xi}$ in the following fashion

$$\begin{aligned} T\mathrm{Grad}_Y \boldsymbol{\xi} &= (T\mathrm{Grad}_Y \boldsymbol{\xi})_{ABCD} \boldsymbol{e}_A \otimes \boldsymbol{e}_B \otimes \boldsymbol{e}_C \otimes \boldsymbol{e}_D \\ &= (\mathrm{Grad}_Y \boldsymbol{\xi})_{ACDB} \boldsymbol{e}_A \otimes \boldsymbol{e}_B \otimes \boldsymbol{e}_C \otimes \boldsymbol{e}_D \\ &= \frac{\partial \xi_{ACD}}{\partial Y_B} \boldsymbol{e}_A \otimes \boldsymbol{e}_B \otimes \boldsymbol{e}_C \otimes \boldsymbol{e}_D. \end{aligned} \tag{44}$$

The cell problem for $\boldsymbol{\omega}$ is given by

$$\begin{cases} \mathrm{Div}_Y \left[\mathscr{C}_{\mathrm{R}} : \mathrm{Grad}_Y \boldsymbol{\omega} - \mathrm{Grad}_Y \boldsymbol{\omega} (\mathscr{C}_{\mathrm{R}} : \boldsymbol{E}_{\mathrm{p}}^{(0)}) \right] & \\ \quad = \mathrm{Div}_Y \left[\mathscr{C}_{\mathrm{R}} : \boldsymbol{E}_{\mathrm{p}}^{(0)} \right], & \text{in } \mathcal{Y}_0 \setminus \Gamma_0 \times \mathcal{T}, \\ [\![\boldsymbol{\omega}]\!] = \boldsymbol{0}, & \text{on } \Gamma_0 \times \mathcal{T}, \\ [\![\left(\mathscr{C}_{\mathrm{R}} : \mathrm{Grad}_Y \boldsymbol{\omega} - \mathrm{Grad}_Y \boldsymbol{\omega} (\mathscr{C}_{\mathrm{R}} : \boldsymbol{E}_{\mathrm{p}}^{(0)}) \right. & \\ \quad \left. - \mathscr{C}_{\mathrm{R}} : \boldsymbol{E}_{\mathrm{p}}^{(0)} \right) \cdot \boldsymbol{N}_{\mathcal{Y}}]\!] = \boldsymbol{0}, & \text{on } \Gamma_0 \times \mathcal{T}. \end{cases} \tag{45}$$

By virtue of the linearization process, we obtain two auxiliary cell problems where the macroscopic term $\mathrm{Grad}_X \boldsymbol{u}^{(0)}$ is not explicitly present. Indeed, this is in general possible only when accounting for the linearized deformations' regime, see also [15]. Then, the dependence of the macro-scale variable is given through the tensor $\boldsymbol{F}_{\mathrm{p}}^{(0)}$, which describes the plastic-like distortions. Moreover, if $\boldsymbol{F}_{\mathrm{p}}^{(0)}$ only depends on time, as is the case in [2], the cell problems are also decoupled in the spatial micro- and macro-variables provided that the elasticity tensor solely depends on the microscale variable. The cell problems are in any case time-dependent, as they encode the evolution of the material response and its link with the plastic-like distortions.

Homogenized problem. From (36) and (42), the homogenized problem rewrites

$$\begin{cases} \mathrm{Div}_X\big[\hat{\mathscr{C}}_{\mathrm{R}} : \mathrm{Grad}_X \boldsymbol{u}^{(0)}\big] = -\mathrm{Div}_X\big[\hat{\boldsymbol{D}}_{\mathrm{R}}\big], & \text{in } \mathcal{B}_h \times \mathcal{T}, \\ (\hat{\mathscr{C}}_{\mathrm{R}} : \mathrm{Grad}_X \boldsymbol{u}^{(0)}) \cdot \boldsymbol{N} + \hat{\boldsymbol{D}}_{\mathrm{R}} \cdot \boldsymbol{N} = \bar{\boldsymbol{T}}, & \text{on } \partial_T \mathcal{B}_h \times \mathcal{T}, \\ \boldsymbol{u}^{(0)} = \bar{\boldsymbol{u}}, & \text{on } \partial_u \mathcal{B}_h \times \mathcal{T}, \end{cases} \tag{46}$$

where

$$\hat{\mathscr{C}}_{\mathrm{R}} = \big\langle \mathscr{C}_{\mathrm{R}} + \mathscr{C}_{\mathrm{R}} : T\mathrm{Grad}_Y \boldsymbol{\xi} - T\mathrm{Grad}_Y \boldsymbol{\xi} (\mathscr{C}_{\mathrm{R}} : \boldsymbol{E}_{\mathrm{p}}^{(0)}) - \boldsymbol{I} \underline{\otimes} (\mathscr{C}_{\mathrm{R}} : \boldsymbol{E}_{\mathrm{p}}^{(0)}) \big\rangle, \tag{47a}$$

$$\hat{\boldsymbol{D}}_{\mathrm{R}} = \big\langle \mathscr{C}_{\mathrm{R}} : \mathrm{Grad}_Y \boldsymbol{\omega} - \mathrm{Grad}_Y \boldsymbol{\omega} (\mathscr{C}_{\mathrm{R}} : \boldsymbol{E}_{\mathrm{p}}^{(0)}) - \mathscr{C}_{\mathrm{R}} : \boldsymbol{E}_{\mathrm{p}}^{(0)} \big\rangle. \tag{47b}$$

Remark 3. *In the absence of distortions, that is for $\boldsymbol{F}_{\mathrm{p}}^{\varepsilon} = \boldsymbol{I}$, the cell problems* (43) *and* (45) *reduce to one single cell problem,*

$$\begin{cases} \mathrm{Div}_Y[\mathscr{C} + \mathscr{C} : T\mathrm{Grad}_Y \boldsymbol{\xi}] = \boldsymbol{0}, & \textit{in } \mathcal{Y}_0 \setminus \Gamma_0 \times \mathcal{T}, \\ [\![\boldsymbol{\xi}]\!] = \boldsymbol{0}, & \textit{on } \Gamma_0 \times \mathcal{T}, \\ [\![(\mathscr{C} + \mathscr{C} : T\mathrm{Grad}_Y \boldsymbol{\xi}) \cdot \boldsymbol{N}_{\mathcal{Y}}]\!] = \boldsymbol{0}, & \textit{on } \Gamma_0 \times \mathcal{T}. \end{cases} \tag{48}$$

This is due to the fact that the symmetric tensor $\boldsymbol{E}_{\mathrm{p}}^{(0)}$ appearing in (40) *is equal to zero. On the other hand, the homogenized problem is rewritten as follows,*

$$\begin{cases} \mathrm{Div}_X[\hat{\mathscr{C}} : \mathrm{Grad}_X \boldsymbol{u}^{(0)}] = \boldsymbol{0}, & \textit{in } \mathcal{B}_h \times \mathcal{T}, \\ (\hat{\mathscr{C}} : \mathrm{Grad}_X \boldsymbol{u}^{(0)}) \cdot \boldsymbol{N} = \bar{\boldsymbol{T}}, & \textit{on } \partial_T \mathcal{B}_h \times \mathcal{T}, \\ \boldsymbol{u}^{(0)} = \bar{\boldsymbol{u}}, & \textit{on } \partial_u \mathcal{B}_h \times \mathcal{T}, \end{cases} \tag{49}$$

where $\hat{\mathscr{C}} = \langle \mathscr{C} + \mathscr{C} : T\mathrm{Grad}_Y \boldsymbol{\xi} \rangle$ *is the effective elasticity tensor. Formulations* (48) *and* (49) *are the counterparts of* (24) *and* (25)*, respectively, when plastic-like distortions are neglected and a linearized approach for the deformations is considered. Particularly,* (48) *and* (49) *identify identically with classical results in the asymptotic homogenization literature [5, 77].*

5.2. Evolution law

Several procedures can be adopted to establish a proper evolution law for the inelastic distortions. One choice is to follow a phenomenological approach, which should be based on experimental evidences and comply with suitable constitutive requirements [29]. On the other hand, one could invoke some general principles, such as the invariance of the evolution law with respect to a class of transformations and thermodynamic constraints [21, 22, 23]. Within the latter approach, and adapting the theoretical framework explored in [21, 22, 23, 29], an evolution equation for the inelastic distortions has been studied in [19]. Therein, the plastic-like distortions describe a remodeling process with the following assumptions: (i) $\boldsymbol{F}_{\mathrm{p}}$ is restricted by the constraint $J_{\mathrm{p}} = 1$, (ii) the solid phase exhibits hyperelastic behavior, and (iii) the considered system remodels when the stress induced by external loading exceeds a characteristic threshold. An evolution law for $\boldsymbol{F}_{\mathrm{p}}$ satisfying these conditions, and compatible with the Dissipation inequality [12, 32, 33, 34], is given by

$$\mathrm{sym}\left(\boldsymbol{C}\boldsymbol{F}_{\mathrm{p}}^{-1}\dot{\boldsymbol{F}}_{\mathrm{p}}\right) = \gamma \left[\|\mathrm{dev}\boldsymbol{\sigma}\| - \sqrt{\tfrac{2}{3}}\sigma_y\right]_+ \frac{\mathrm{dev}(\boldsymbol{\Sigma})\boldsymbol{C}}{\|\mathrm{dev}\boldsymbol{\sigma}\|}, \tag{50}$$

where $\boldsymbol{\sigma}$ is the Cauchy stress tensor, $\mathrm{dev}(\boldsymbol{\Sigma}) = \boldsymbol{\Sigma} - \frac{1}{3}\mathrm{tr}(\boldsymbol{\Sigma})\boldsymbol{I}$, is the deviatoric part of the Mandell stress tensor $\boldsymbol{\Sigma} = \boldsymbol{C}\boldsymbol{S}$ being the Mandel stress tensor, and $\boldsymbol{S} = \boldsymbol{F}^{-1}\boldsymbol{T}$ the second Piola-Kirchhoff stress tensor. Moreover, γ is a strictly positive model parameter, $\sigma_y > 0$ is the yield, or threshold, stress, and the operator $[A]_+$ is such that, for any real number A, $[A]_+ = A$, if $A > 0$, and $[A]_+ = 0$ otherwise. As anticipated in the Introduction, in the present context the physical meaning of the plastic-like distortions, represented by $\boldsymbol{F}_{\mathrm{p}}$, is that of structural reorganization, i.e. remodeling, as is the case in biological tissues when the adhesion bonds among cells or the structure of the ECM reorganize themselves.

Although Equation (50) has been successfully used to describe some biological situations in which the onset of remodeling is subordinated to the excess of the yield stress σ_y, the homogenization of the evolution law (50) is too complicated. For this reason, in this work, we replace (50) with a much easier law of the type

$$\mathrm{sym}\left(\boldsymbol{C}(\boldsymbol{F}_{\mathrm{p}})^{-1}\dot{\boldsymbol{F}}_{\mathrm{p}}\right) = \gamma\,\mathrm{dev}(\boldsymbol{\Sigma})\boldsymbol{C}, \tag{51}$$

according to which no stress-activation criterion is supplied. Clearly, this choice may turn out to be unrealistic in many circumstances, but it can still be useful to understand the essence of some stress-driven remodeling processes.

We need to clarify that, although in some sentences of this work we mentioned growth, our model focuses on *pure* remodeling. This is reflected by the condition $\det\boldsymbol{F}_{\mathrm{p}} = 1$, and, more importantly, by the fact that the evolution laws (50) and (51) are triggered and controlled exclusively by mechanical factors. On the one hand, the requirement $\det\boldsymbol{F}_{\mathrm{p}} = 1$ means that the plastic-like distortions are isochoric and, thus, unable to describe volumetric growth. On the other hand, the evolution laws for $\boldsymbol{F}_{\mathrm{p}}$, i.e., Eqs. (50) or (51), imply that remodeling is viewed as a consequence of the mechanical environment only: When mechanical stress exceeds a given threshold (see also [29, 34]), the internal structure of the tissue starts to vary. In other words, in the present framework, no biochemical phenomena are accounted for as possible activators of remodeling. This is a remarkable difference with growth, which, in contrast, occurs only when the concentration of nutrients is above a certain threshold value [2, 10, 3, 26, 52]. Our results do not apply to growth as they stand, nonetheless, the theory can be adapted to model growth by doing some necessary modifications. This is the reason why in the abstract we stated that our study offers *"a robust framework that can be readily generalized to growth and remodeling of nonlinear composites"*.

To homogenize (51), the first step is to rewrite it as

$$\mathrm{sym}\left(\boldsymbol{C}^{\varepsilon}(\boldsymbol{F}_{\mathrm{p}}^{\varepsilon})^{-1}\dot{\boldsymbol{F}}_{\mathrm{p}}^{\varepsilon}\right) = \gamma^{\varepsilon}\mathrm{dev}(\boldsymbol{\Sigma}^{\varepsilon})\boldsymbol{C}^{\varepsilon}, \tag{52}$$

by admitting that $\gamma^{\varepsilon}(X) = \gamma(X, Y)$ is a rapidly oscillating strictly positive function. Moreover, by performing the power expansion for $\boldsymbol{\Sigma}^{\varepsilon}$,

$$\boldsymbol{\Sigma}^{\varepsilon}(X,t) = \sum_{k=0}^{+\infty} \boldsymbol{\Sigma}^{(k)}(X,Y,t)\varepsilon^{k}\,, \tag{53}$$

and using (31), the leading order term of $\boldsymbol{\Sigma}^{\varepsilon}$ is

$$\boldsymbol{\Sigma}^{(0)} = \boldsymbol{C}^{(0)}\big[\mathscr{C}_{\mathrm{R}} : (\boldsymbol{E}^{(0)} - \boldsymbol{E}_{\mathrm{p}}^{(0)})\big]. \tag{54}$$

In the limit of small elastic deformations, in (54) we must neglect non-linear terms in $\boldsymbol{H}$. Therefore, $\boldsymbol{\Sigma}^{(0)}$ is approximated with

$$\boldsymbol{\Sigma}_{\mathrm{lin}}^{(0)} = \mathscr{C}_{\mathrm{R}} : \mathrm{sym}\boldsymbol{H} - \big(\boldsymbol{I} + 2\mathrm{sym}\boldsymbol{H}\big)\big(\mathscr{C}_{\mathrm{R}} : \boldsymbol{E}_{\mathrm{p}}^{(0)}\big).$$

By virtue of (12a), $\mathrm{sym}\boldsymbol{H}$ splits additively as the sum of

$$\mathrm{sym}\boldsymbol{H} = \boldsymbol{E}_{X}^{(0)} + \boldsymbol{E}_{Y}^{(1)}, \tag{55}$$

where, for $k = 0, 1$, and $j_k = X, Y$,

$$\boldsymbol{E}_{j_k}^{(k)} = \tfrac{1}{2}\big[\mathrm{Grad}_{j_k}\boldsymbol{u}^{(k)} + (\mathrm{Grad}_{j_k}\boldsymbol{u}^{(k)})^{T}\big]. \tag{56}$$

By using (55) and (42), we can now rewrite $\boldsymbol{\Sigma}_{\mathrm{lin}}^{(0)}$ as

$$\boldsymbol{\Sigma}_{\mathrm{lin}}^{(0)} = \mathscr{A}_{\mathrm{R}} : \mathrm{Grad}_{X}\boldsymbol{u}^{(0)} + \mathscr{B}_{\mathrm{R}} : \mathrm{Grad}_{Y}\boldsymbol{\omega} - \mathscr{C}_{\mathrm{R}} : \boldsymbol{E}_{\mathrm{p}}^{(0)}, \tag{57}$$

with

$$\begin{aligned} \mathscr{A}_{\mathrm{R}} = \mathscr{C}_{\mathrm{R}} &+ \mathscr{C}_{\mathrm{R}} : T\mathrm{Grad}_{Y}\boldsymbol{\xi} - \boldsymbol{I}\,\overline{\underline{\otimes}}(\mathscr{C}_{\mathrm{R}} : \boldsymbol{E}_{\mathrm{p}}^{(0)}) \\ &+ \big[\boldsymbol{I}\,\underline{\otimes}(\mathscr{C}_{\mathrm{R}} : \boldsymbol{E}_{\mathrm{p}}^{(0)})\big] : \big[T\mathrm{Grad}_{Y}\boldsymbol{\xi} + {}^{t}(T\mathrm{Grad}_{Y}\boldsymbol{\xi})\big], \end{aligned} \tag{58a}$$

$$\mathscr{B}_{\mathrm{R}} = \mathscr{C}_{\mathrm{R}} + \boldsymbol{I}\,\overline{\underline{\otimes}}(\mathscr{C}_{\mathrm{R}} : \boldsymbol{E}_{\mathrm{p}}^{(0)}). \tag{58b}$$

In Equation (58a), the symbol ${}^{t}(\bullet)$ transposes the fourth-order tensor to which it is applied by exchanging the order of its first pair of indices only, i.e., given an arbitrary fourth-order tensor $\mathscr{T} = \mathscr{T}_{ABCD}\boldsymbol{e}_A \otimes \boldsymbol{e}_B \otimes \boldsymbol{e}_C \otimes \boldsymbol{e}_D$, ${}^{t}\mathscr{T}$ reads

$${}^{t}\mathscr{T} = \mathscr{T}_{BACD}\boldsymbol{e}_A \otimes \boldsymbol{e}_B \otimes \boldsymbol{e}_C \otimes \boldsymbol{e}_D. \tag{59}$$

Note that in the calculations performed to obtain $\mathscr{A}_{\mathrm{R}}$ and $\mathscr{B}_{\mathrm{R}}$ in (57), we employed the following properties: given two second-order tensors $\boldsymbol{A}$ and $\boldsymbol{U}$, with $\boldsymbol{A}$ being symmetric, it holds that

$$\boldsymbol{U}\boldsymbol{A} = (\boldsymbol{I}\,\underline{\otimes}\boldsymbol{A}) : \boldsymbol{U}, \tag{60a}$$

$$\boldsymbol{U}^{T}\boldsymbol{A} = (\boldsymbol{I}\,\overline{\otimes}\boldsymbol{A}) : \boldsymbol{U}. \tag{60b}$$

Finally, by substituting the expansions of $\boldsymbol{\Sigma}^{\varepsilon}$ and $\boldsymbol{F}_{\rm p}^{\varepsilon}$ in (52), equating the leading order terms, excluding non-linear terms of $\boldsymbol{H}$ and averaging, the homogenized evolution law for the plastic-like distortions is

$$\mathrm{sym}\big[\langle \boldsymbol{C}_{\rm lin}^{(0)}(\boldsymbol{F}_{\rm p}^{(0)})^{-1}\dot{\overline{\boldsymbol{F}_{\rm p}^{(0)}}}\rangle\big] = -\big\langle \gamma \mathrm{dev}(\boldsymbol{\Sigma}_{\rm lin}^{(0)})\big\rangle - \big\langle \gamma(\mathscr{C}_{\rm R} : \boldsymbol{E}_{\rm p}^{(0)})(\boldsymbol{C}_{\rm lin}^{(0)} - \boldsymbol{I})\big\rangle, \quad (61)$$

where $\boldsymbol{\Sigma}_{\rm lin}^{(0)}$ is given in (57) and

$$\begin{aligned}\boldsymbol{C}_{\rm lin}^{(0)} &= \boldsymbol{I} + 2\mathrm{sym}\boldsymbol{H} \\ &= \boldsymbol{I} + 2(\mathscr{I} + \mathscr{I} : T\mathrm{Grad}_Y\boldsymbol{\xi}) : \mathrm{Grad}_X\boldsymbol{u}^{(0)} + 2\mathscr{I} : \mathrm{Grad}_Y\boldsymbol{\omega}. \quad (62)\end{aligned}$$

We note that, to compute $\boldsymbol{C}_{\rm lin}^{(0)}$, we must first determine $\boldsymbol{\xi}$ and $\boldsymbol{\omega}$, which is done by solving the local problems (43) and (45). Furthermore, Equation (61) needs to be supplemented with an initial condition for $\boldsymbol{F}_{\rm p}^{(0)}$.

Remark 4. *In the linearized theory of elasticity, even when the individual constituents of a given composite material are isotropic, the effective elastic coefficients may turn out to be anisotropic, depending on the geometric properties of the micro-structure. In fact, when the Homogenization Theory is applied, the anisotropy arises quite naturally due to the solution of the local cell problems [5, 8]. In fact, the homogenized material is anisotropic also in the case of rather simple cells, see for instance [61], where an explicit deviation-from- isotropy function is introduced in the context of cubic symmetric elasticity tensors arising from asympototic homogenization. This has noticeable repercussions also on the evolution law that should be chosen for a correct description of remodeling. To see this, we first notice that, for an isotropic medium, the evolution law of the plastic-like distortions can be formulated in terms of tensor* $\boldsymbol{B}_{\rm p}$*, since the constitutive framework is such that* $\boldsymbol{F}_{\rm p}$ *does not feature explicitly in any constitutive function (see e.g. [78]). In such cases, a possible evolution law for* $\boldsymbol{B}_{\rm p}$ *may be given in the form*

$$\dot{\boldsymbol{B}}_{\rm p} = \gamma \boldsymbol{B}_{\rm p}\mathrm{dev}(\boldsymbol{\Sigma}). \quad (63)$$

Equation (63) *is, in fact, in harmony with the symmetry properties of the material Mandel stress tensor,* $\boldsymbol{\Sigma}$*, i.e.,* $\boldsymbol{B}_{\rm p}\boldsymbol{\Sigma} = (\boldsymbol{B}_{\rm p}\boldsymbol{\Sigma})^T$ *[54]. However, if one writes an equation of the same type as* (63) *at the scale of a cell problem (which seems to be a justified choice, because the material is isotropic at that scale), and then homogenizes, one ends up with a material for which* *the Mandel stress tensor* $\boldsymbol{\Sigma}$ *no longer obeys the symmetry condition* $\boldsymbol{B}_{\rm p}\boldsymbol{\Sigma} = (\boldsymbol{B}_{\rm p}\boldsymbol{\Sigma})^T$. *This is because the material is not isotropic at the macroscale and, thus, the description of remodeling based on* $\boldsymbol{B}_{\rm p}$ *becomes inadequate. Therefore, if one wants to homogenize, one should start with evolution laws at the microscale, which have to be suitable to account for anisotropy, even though the single constituents are isotropic at that scale. These considerations lead us to Equation* (52)*, as suggested in [22, 23], and subsequently employed in [19].*

Remark 5. *Equations* (50) *and* (51) *can be obtained by adhering to the philosophy presented in [12, 18], and subsequently adopted, for example, in [3] for growth, in [44] for growth and remodeling, and in [31, 32] for remodeling only. Accordingly,* $\boldsymbol{F}_{\rm p}$ *is regarded as the kinematic descriptor of the structural degrees of freedom of the medium, and* $\dot{\boldsymbol{F}}_{\rm p}$ *as the generalized velocity with which the structural changes occur. Within this setting, it can be proven that for growth and remodeling problems, the dissipation inequality reads*

$$\mathcal{D} = \boldsymbol{Y}_\nu : \boldsymbol{L}_{\rm p} + \mathcal{D}_{\rm nc} \geq 0, \tag{64}$$

where $\mathcal{D}_{\rm mech} := \boldsymbol{Y}_\nu : \boldsymbol{L}_{\rm p}$ *is the* mechanical contribution *to dissipation, with* $\boldsymbol{Y}_\nu$ *being the dissipative part of a generalized internal force, dual to* $\boldsymbol{L}_{\rm p}$*. In our work, however,* $\boldsymbol{Y}_\nu$ *can be identified with the tensor* $\boldsymbol{Y}_\nu \equiv J_{\rm p}^{-1}\boldsymbol{F}_{\rm p}^{-{\rm T}}\boldsymbol{\Sigma}\boldsymbol{F}_{\rm p}^{\rm T}$*, so that* $\mathcal{D}_{\rm mech}$ *coincides with the mechanical dissipation encountered in the standard formulation of Elastoplasticity, i.e.,* $\mathcal{D}_{\rm mech} = J_{\rm p}^{-1}\boldsymbol{F}_{\rm p}^{-{\rm T}}\boldsymbol{\Sigma}\boldsymbol{F}_{\rm p}^{\rm T} : \boldsymbol{L}_{\rm p} = J_{\rm p}^{-1}\boldsymbol{\Sigma} : \boldsymbol{F}_{\rm p}^{-1}\dot{\boldsymbol{F}}_{\rm p}$.

In the terminology of [45, 30], $\mathcal{D}_{\rm nc}$ *is referred to as "*non-compliant*" contribution to the overall dissipation. Physically, it summarizes a class of phenomena that are not —or cannot be— resolved in terms of mechanical power at the scale at which the dissipation inequality is written. For instance, in the case of growth,* $\mathcal{D}_{\rm nc}$ *may represent biochemical effects contributing to the overall dissipation.*

The inequality (64) *can be studied in several ways, depending on the problem at hand. First, we consider a growth problem. To this end, we assume that* $\mathcal{D}_{\rm nc}$ *can be written as* $\mathcal{D}_{\rm nc} = r\mathcal{A}$*, where* r *is the rate at which mass is added or depleted from the system (its units are given by the reciprocal of time), and* $\mathcal{A}$ *is the energy density (per unit volume) associated with the introduction or uptake of mass. In this setting, it is possible to conceive a particular state of the system in which the* mechanical *stress is null, i.e.,* $\boldsymbol{\Sigma} = \boldsymbol{0}$*, while* r *and* $\mathcal{A}$ *are generally nonzero. When this occurs, the system* *grows without mechanical dissipation, i.e.,* $\mathcal{D}_{\text{mech}} = 0$*, whereas the overall dissipation of the system reduces to the non-compliant one:*

$$\mathcal{D} \equiv \mathcal{D}_{\text{nc}} = r\mathcal{A} \geq 0. \tag{65}$$

The second case addresses the situation of pure remodeling, for which we set $\mathcal{D}_{\text{nc}} = 0$*, so that the dissipation inequality* (64) *becomes*

$$\mathcal{D} = \mathcal{D}_{\text{mech}} = \boldsymbol{Y}_{\nu} : \boldsymbol{L}_{\text{p}} = J_{\text{p}}^{-1}\boldsymbol{\Sigma} : \boldsymbol{F}_{\text{p}}^{-1}\dot{\boldsymbol{F}}_{\text{p}} \geq 0. \tag{66}$$

It is possible to show that the evolution laws (50) *and* (51) *are in harmony with* (66)*.*

6. A computational scheme for small deformations

The macro-scale model given by the problems (46) and (61), together with the auxiliary cell problems (43) and (45), requires dedicated numerical schemes which are subject of our current investigations. The main computational challenge is due to the fact that the local problems depend on the macro-scale in a time-dependent way. Therefore, at each time, there is a different cell problem at each macroscopic point $X \in \mathcal{B}_h$. Moreover, one has to transfer the information (represented by the geometry, material coefficients, and unknowns of the problem) from the cell problems to the homogenized problem in the domain $\mathcal{B}_h$, and vice versa.

Here, as a first step towards the numerical study of this kind of problems, we propose an algorithm adapted from [31] that could be useful in our case. In [31] it is introduced a computational algorithm, named Generalised Plasticity Algorithm (GPA), to study the mechanical response of a biological tissue that undergoes large deformations and remodeling of its internal structure. Following [31], the discrete and linearized version of the problem constituted by Equations (43), (45), (46) and (61) is formulated in three steps.

First step. The weak form of the cell problems (43) and (45), and of the homogenized problem (46) can be *formally* rewritten as

$$\mathcal{L}_1^w(\boldsymbol{\xi}, \boldsymbol{F}_{\text{p}}^{(0)}, \tilde{\boldsymbol{\xi}}) = 0, \tag{67a}$$

$$\mathcal{L}_2^w(\boldsymbol{\omega}, \boldsymbol{F}_{\text{p}}^{(0)}, \tilde{\boldsymbol{\omega}}) = 0, \tag{67b}$$

$$\mathcal{H}_1^w(\boldsymbol{u}^{(0)}, \boldsymbol{F}_{\text{p}}^{(0)}, \tilde{\boldsymbol{u}}^{(0)}) = 0, \tag{67c}$$

where $\tilde{\boldsymbol{\xi}}$, $\tilde{\boldsymbol{\omega}}$ and $\tilde{\boldsymbol{u}}^{(0)}$ are test functions defined in certain Sobolev spaces, and $\mathcal{L}_1^w$, $\mathcal{L}_2^w$ and $\mathcal{H}_1^w$ are suitable integral operators. Together with (67a)-(67c), we rewrite in operatorial form also the homogenized problem (61) as

$$\mathcal{H}_2(\boldsymbol{\xi}, \boldsymbol{\omega}, \boldsymbol{u}^{(0)}, \boldsymbol{F}_{\mathrm{p}}^{(0)}) = \mathbf{0}. \tag{68}$$

Note that (68) is not a weak form because the corresponding equation does not involved spatial derivatives of $\boldsymbol{F}_{\mathrm{p}}^{(0)}$.

Second step. We perform a backward Euler method [78] for discretizing the evolution law for $\boldsymbol{F}_{\mathrm{p}}^{(0)}$ given by (68), thereby ending up with the following system of time-discrete equations,

$$\mathcal{L}_{1[n]}^w(\boldsymbol{\xi}_{[n]}, \boldsymbol{F}_{\mathrm{p}[n]}^{(0)}, \tilde{\boldsymbol{\xi}}) = 0, \tag{69a}$$

$$\mathcal{L}_{2[n]}^w(\boldsymbol{\omega}_{[n]}, \boldsymbol{F}_{\mathrm{p}[n]}^{(0)}, \tilde{\boldsymbol{\omega}}) = 0, \tag{69b}$$

$$\mathcal{H}_{1[n]}^w(\boldsymbol{u}_{[n]}^{(0)}, \boldsymbol{F}_{\mathrm{p}[n]}^{(0)}, \tilde{\boldsymbol{u}}^{(0)}) = 0, \tag{69c}$$

$$\mathcal{H}_{2[n]}(\boldsymbol{\xi}_{[n]}, \boldsymbol{\omega}_{[n]}, \boldsymbol{u}_{[n]}^{(0)}, \boldsymbol{F}_{\mathrm{p}[n]}^{(0)}) = \mathbf{0}, \tag{69d}$$

where $n = 1, \ldots, N$ enumerates the nodes of a suitable time grid. We notice that an explicit time discrete method could be also used. However, when dealing with problems in Elastoplasticity, this election could lead to a less accurate solution.

Third step. The operators $\mathcal{L}_{1[n]}^w$, $\mathcal{L}_{2[n]}^w$, $\mathcal{H}_{1[n]}^w$ and $\mathcal{H}_{2[n]}$, are linear in $\boldsymbol{\xi}_{[n]}$, $\boldsymbol{\omega}_{[n]}$ and $\boldsymbol{u}_{[n]}^{(0)}$, respectively, but they are nonlinear in $\boldsymbol{F}_{\mathrm{p}[n]}^{(0)}$. Thus, to search the solution to (69a)-(69d), we linearize at each time step according to Newton's method (with a linesearch). Therefore, at the kth iteration, $k \in \mathbb{N}$, $k \geq 1$, $\boldsymbol{F}_{\mathrm{p}[n,k]}^{(0)}$ is written as

$$\boldsymbol{F}_{\mathrm{p}[n,k]}^{(0)} = \boldsymbol{F}_{\mathrm{p}[n,k-1]}^{(0)} + \boldsymbol{\Psi}_{[n,k]}, \tag{70}$$

where $\boldsymbol{F}_{\mathrm{p}[n,k-1]}^{(0)}$ is known and $\boldsymbol{\Psi}_{[n,k]}$ represents the unknown increment. We introduce the notation

$$\mathcal{L}_{1[n,k-1]}^w(\boldsymbol{\xi}_{[n]}, \tilde{\boldsymbol{\xi}}) = \mathcal{L}_{1[n]}^w(\boldsymbol{\xi}_{[n]}, \boldsymbol{F}_{\mathrm{p}[n,k-1]}^{(0)}, \tilde{\boldsymbol{\xi}}), \tag{71a}$$

$$\mathcal{L}_{2[n,k-1]}^w(\boldsymbol{\omega}_{[n]}, \tilde{\boldsymbol{\omega}}) = \mathcal{L}_{2[n]}^w(\boldsymbol{\omega}_{[n]}, \boldsymbol{F}_{\mathrm{p}[n,k-1]}^{(0)}, \tilde{\boldsymbol{\omega}}), \tag{71b}$$

$$\mathcal{H}_{1[n,k-1]}^w(\boldsymbol{u}_{[n]}^{(0)}, \tilde{\boldsymbol{u}}_{[n]}^{(0)}) = \mathcal{H}_{1[n]}^w(\boldsymbol{u}_{[n]}^{(0)}, \boldsymbol{F}_{\mathrm{p}[n,k-1]}^{(0)}, \tilde{\boldsymbol{u}}_{[n]}^{(0)}). \tag{71c}$$

Now, for each time step, and at the kth iteration, we solve

$$\mathcal{L}^{w}_{1[n,k-1]}(\boldsymbol{\xi}_{[n]}, \tilde{\boldsymbol{\xi}}) = 0, \tag{72a}$$

$$\mathcal{L}^{w}_{2[n,k-1]}(\boldsymbol{\omega}_{[n]}, \tilde{\boldsymbol{\omega}}) = 0, \tag{72b}$$

$$\mathcal{H}^{w}_{1[n,k-1]}(\boldsymbol{u}^{(0)}_{[n]}, \tilde{\boldsymbol{u}}^{(0)}) = 0, \tag{72c}$$

and obtain the "temporary" solutions $\boldsymbol{\xi}_{[n,k-1]}$, $\boldsymbol{\omega}_{[n,k-1]}$, and $\boldsymbol{u}^{(0)}_{[n,k-1]}$, respectively. Then, upon setting

$$\mathcal{H}_{2[n,k-1]} = \mathcal{H}_{2[n]}(\boldsymbol{\xi}_{[n,k-1]}, \boldsymbol{\omega}_{[n,k-1]}, \boldsymbol{u}^{(0)}_{[n,k-1]}, \boldsymbol{F}^{(0)}_{\mathrm{p}[n,k-1]}), \tag{73a}$$

$$\mathscr{H}_{[n,k-1]} = \mathscr{H}_{[n]}(\boldsymbol{\xi}_{[n,k-1]}, \boldsymbol{\omega}_{[n,k-1]}, \boldsymbol{u}^{(0)}_{[n,k-1]}, \boldsymbol{F}^{(0)}_{\mathrm{p}[n,k-1]}), \tag{73b}$$

we linearize (69d), i.e.,

$$\mathcal{H}_{2[n,k-1]} + \mathscr{H}_{[n,k-1]} : \boldsymbol{\Psi}_{[n,k]} = \boldsymbol{0}, \tag{74}$$

where $\mathscr{H}_{[n,k-1]}$ is a fourth-order tensor given by the Gâteaux derivative of $\mathcal{H}_{2[n]}$, computed with respect to its fourth argument, and evaluated in $\boldsymbol{F}^{(0)}_{\mathrm{p}[n,k-1]}$.

If the residuum $\boldsymbol{F}^{(0)}_{\mathrm{p}[n,k]}$ for k greater than, or equal to, a certain k_* is less than a tolerance $\delta > 0$, then we set $\boldsymbol{F}^{(0)}_{\mathrm{p}[n]} \equiv \boldsymbol{F}^{(0)}_{\mathrm{p}[n,k_*]} = \boldsymbol{F}^{(0)}_{\mathrm{p}[n,k_*-1]} + \boldsymbol{\Psi}_{[n,k_*]}$ and we regard it as the solution of Newton's method. Thus, we compute $\boldsymbol{\xi}_{[n]}$, $\boldsymbol{\omega}_{[n]}$ and $\boldsymbol{u}^{(0)}_{[n]}$.

These three steps are summarized in the algorithm 1.

7. Numerical results

In this section, the potentiality of our model, which is given by Equations (43), (45), (46) and (61), is shown by performing numerical simulations. In particular, we make the following considerations.

(i) Geometry. We consider the composite body $\mathcal{B}^{\varepsilon}$ to have a layered three-dimensional structure, and we assume that the layers are orthogonal to the direction $\boldsymbol{\mathcal{E}}_3$, where $\{\boldsymbol{\mathcal{E}}_A\}_{A=1}^{3}$ is an orthonormal basis of a system of Cartesian coordinates $\{X_A\}_{A=1}^{3}$. In this particular case, the material properties of the heterogeneous body only change along the $\boldsymbol{\mathcal{E}}_3$ direction and, thus, they depend solely on the coordinate X_3. Consequently, the benchmark test at

Algorithm 1

procedure
  for $n = 1, \ldots, N$ **do**
    State $k = 1$
    while $e > \delta$ **do** *(Known* $\boldsymbol{F}^{(0)}_{\mathrm{p}[n,k-1]}$*)*
      Solve $\mathcal{L}^{w}_{1[n,k-1]}$ and $\mathcal{L}^{w}_{2[n,k-1]}$ *(To find* $\boldsymbol{\xi}_{[n,k-1]}$ *and* $\boldsymbol{\omega}_{[n,k-1]}$*)*
      Solve $\mathcal{H}^{w}_{1[n,k-1]}$ *(To find* $\boldsymbol{u}^{(0)}_{[n,k-1]}$*)*
      Solve $\mathcal{H}^{w}_{1[n,k-1]}$ *(To find* $\boldsymbol{\Psi}_{[n,k]}$*)*
      $\boldsymbol{F}^{(0)}_{\mathrm{p}[n,k-1]} \leftarrow \boldsymbol{F}^{(0)}_{\mathrm{p}[n,k-1]} + \boldsymbol{\Psi}_{[n,k]}$
      Compute e
      $k = k + 1$
    end while
    $\boldsymbol{F}^{(0)}_{\mathrm{p}[n]} = \boldsymbol{F}^{(0)}_{\mathrm{p}[n,k-1]} + \boldsymbol{\Psi}_{[n,k]}$
    Solve $\mathcal{L}^{w}_{1[n]}$ and $\mathcal{L}^{w}_{2[n]}$ *(To find* $\boldsymbol{\xi}_{[n]}$ *and* $\boldsymbol{\omega}_{[n]}$*)*
    Solve $\mathcal{H}^{w}_{1[n]}$ *(To find* $\boldsymbol{u}^{(0)}_{[n]}$*)*
    Update micro and macro geometries
  end for
end procedure

hand can be recast into a one dimensional problem, that is, the reference configuration of the periodic cell and the body are considered to be the unidimensional domains $\mathcal{Y}_0 = [0, \ell]$ and $\mathcal{B}_h = [0, L]$, respectively. We denote with ℓ and L, respectively, the dimension of the periodic cell and the body along the direction $\boldsymbol{\mathcal{E}}_3$. Moreover, we suppose that the interface Γ_0 is the middle point $\ell/2$, so that, each material under consideration has the same volume in the microscopic cell $\mathcal{Y}_0$.

(ii) Material properties. We prescribe the elasticity tensor $\mathscr{C}^{\varepsilon}$ to be independent on the macroscale variable X_3, i.e. $\mathscr{C}^{\varepsilon}(X_3) = \mathscr{C}(X_3, Y_3) \equiv \mathscr{C}(Y_3)$, where $\{Y_A\}_{A=1}^{3}$ is a system of microscale Cartesian coordinates. In addition, as stated above, we consider that the constituents of the heterogeneous material are isotropic, which implies that the non zero components of the 6×6 symmetric matrix representation of $\mathscr{C}$ are given by

$$[\mathscr{C}]_{11} = [\mathscr{C}]_{22} = [\mathscr{C}]_{33} = \lambda + 2\mu, \tag{75a}$$

$$[\mathscr{C}]_{12} = [\mathscr{C}]_{13} = [\mathscr{C}]_{23} = \lambda, \tag{75b}$$

$$[\mathscr{C}]_{44} = [\mathscr{C}]_{55} = [\mathscr{C}]_{66} = \tfrac{1}{2}([\mathscr{C}]_{11} - [\mathscr{C}]_{12}) = \mu, \tag{75c}$$

where λ and μ are Lamé's parameters. We suppose that $\mathscr{C}$ is piece-wise constant, which means that λ and μ are defined as

$$\lambda(Y_3) = \begin{cases} \lambda_1, & \text{in } \mathcal{Y}_0^1 \\ \lambda_2, & \text{in } \mathcal{Y}_0^2 \end{cases} \quad \text{and} \quad \mu(Y_3) = \begin{cases} \mu_1, & \text{in } \mathcal{Y}_0^1 \\ \mu_2, & \text{in } \mathcal{Y}_0^2 \end{cases}. \tag{76}$$

Furthermore, we consider that γ has the same value in both constituents, which means that it is already averaged.

(iii) Plastic-like distortions. We assume that the matrix representation of the tensor $\boldsymbol{F}_{\mathrm{p}}^{(0)}$ is diagonal with non-zero components $[\boldsymbol{F}_{\mathrm{p}}^{(0)}]_{11} = \frac{1}{\sqrt{p}}$, $[\boldsymbol{F}_{\mathrm{p}}^{(0)}]_{22} = \frac{1}{\sqrt{p}}$ and $[\boldsymbol{F}_{\mathrm{p}}^{(0)}]_{33} = p$, where p is defined as the remodeling parameter. Furthermore, we restrict our investigation to the simpler case of $\boldsymbol{F}_{\mathrm{p}}^{(0)}$ depending solely on X_3. This means that, the plastic-like distortions of order ε^0 are, in a sense, already averaged, and thus variable from one cell to the other, not inside them. In other words, we are interested in the production of distortions in the tissue starting from the cell scale, rather than from the cell's microstructure. This, of course, does not mean that the cell's microstructure does not change.

Together the with assumption (ii), we find that the 6×6 matrix representation of the elasticity tensor, pulled-backed to the reference configuration, is symmetric, and its non-zero components are given by

$$[\mathscr{C}_{\mathrm{R}}]_{11} = [\mathscr{C}_{\mathrm{R}}]_{22} = (\lambda + 2\mu)p^2, \qquad [\mathscr{C}_{\mathrm{R}}]_{33} = (\lambda + 2\mu)p^{-4}, \tag{77a}$$

$$[\mathscr{C}_{\mathrm{R}}]_{12} = \lambda p^2, \qquad [\mathscr{C}_{\mathrm{R}}]_{44} = [\mathscr{C}_{\mathrm{R}}]_{55} = \mu p^{-1}, \tag{77b}$$

$$[\mathscr{C}_{\mathrm{R}}]_{13} = [\mathscr{C}_{\mathrm{R}}]_{23} = \lambda p^{-1}, \qquad [\mathscr{C}_{\mathrm{R}}]_{66} = \mu p^2. \tag{77c}$$

We remark that $\mathscr{C}_{\mathrm{R}}$ depends on X_3 and time through p, whereas it inherits the dependence of $\mathscr{C}$ on the micro-scale variable, Y_3.

(iv) Initial and boundary conditions. In the present context, we impose Dirichlet conditions for $\boldsymbol{u}^{(0)}$ on the whole boundary $\partial\mathcal{B}_h$, i.e. we do not consider a Neumann condition and therefore, $\partial_u\mathcal{B}_h \equiv \partial\mathcal{B}_h$. We note that, although the homogenization process was developed for mixed boundary conditions, the whole procedure stands, since the type of boundary conditions does not play a role in the derivation of the homogenized model. In particular, we set $[\boldsymbol{u}^{(0)}]_3 = 0$ at $X_3 = 0$, and $[\boldsymbol{u}^{(0)}]_3 = \frac{u_L t}{t_f}$ at $X_3 = L$, where u_L is a target value for the displacement in the direction $\boldsymbol{\mathcal{E}}_3$. Moreover, we enforce an initial spatial distribution for the remodeling parameter p as $p_{\rm in}(X_3) = \alpha + \beta \cos(\frac{\pi}{L} X_3)$, where α and β are constants, such that $p_{\rm in}(X_3)$ is always strictly positive.

7.1. Discussion of the numerical results

Given the above considerations, we solve the following homogenized equations for $\boldsymbol{u}^{(0)}$ and p,

$$-\frac{\partial}{\partial X_3}([\hat{\mathscr{C}}_{\rm R}]_{i3n3}\frac{\partial[\boldsymbol{u}^{(0)}]_n}{\partial X_3}) = \frac{\partial[\hat{\boldsymbol{D}}_R]_{i3}}{\partial X_3}, \quad \text{for } i = 1,2,3, \tag{78a}$$

$$\langle[\boldsymbol{C}^{(0)}_{\rm lin}]_{33}\rangle\frac{\partial p}{\partial t} = \frac{\gamma}{3}\langle \text{dev}(\boldsymbol{\Sigma}^{(0)}_{\rm lin})\rangle p - \gamma\langle[\mathscr{C}_{\rm R}]_{33nn}[\boldsymbol{E}_{\rm p}]_{nn}([\boldsymbol{C}^{(0)}_{\rm lin}]_{33} - 1)\rangle p, \tag{78b}$$

The coefficients $[\hat{\mathscr{C}}_{\rm R}]_{ijkl}$, $[\hat{\boldsymbol{D}}_R]_{ij}$ and $[\boldsymbol{C}^{(0)}_{\rm lin}]_{ij}$ are given by Equations (47a), (47b) and (62), respectively, and are to be found by solving the auxiliary cell problems for $\boldsymbol{\xi}$ and $\boldsymbol{\omega}$, given by

$$-\frac{\partial}{\partial Y_3}([\mathscr{Q}]_{i3i3}\frac{\partial[\boldsymbol{\xi}]_{ik3}}{\partial Y_3}) = \frac{\partial[\mathscr{Q}]_{i3i3}}{\partial Y_3}\delta_{ik}, \quad \text{for } i,k = 1,2,3, \tag{79a}$$

$$-\frac{\partial}{\partial Y_3}([\mathscr{Q}]_{i3i3}\frac{\partial[\boldsymbol{\omega}]_{i}}{\partial Y_3}) = -\frac{\partial[\boldsymbol{Q}]_{33}}{\partial Y_3}\delta_{i3}, \quad \text{for } i = 1,2,3, \tag{79b}$$

with

$$[\mathscr{Q}]_{i3i3} = [\mathscr{C}_{\rm R}]_{i3i3} - [\boldsymbol{Q}]_{33}, \quad [\boldsymbol{Q}]_{33} = [\mathscr{C}_{\rm R}]_{33nn}[\boldsymbol{E}_{\rm p}]_{nn}. \tag{80a}$$

In this work, we are not interested to address a real world situation. Our aim is, instead, to show how the present theoretical framework can be numerically simulated. For this reason, the parameters used in our computations are arbitrarily chosen (see Table 1).

In Fig. 2, it is plotted the time evolution of the remodeling parameter p at two different points of the macroscopic domain, that is at $X_3 = 7\,\text{cm}$ and $X_3 = 21\,\text{cm}$. We observe that the evolution of p is quite different at these two points. Indeed, at $X_3 = 21\,\text{cm}$, p increases and it is always greater than one. On the contrary, at $X_3 = 7\,\text{cm}$, it is monotonically decreasing and tends to be lower than one. In Fig. 3, we show the spatial profile of the effective coefficients $[\hat{\mathscr{C}}]_{33}$, $[\hat{\mathscr{C}}_{\rm R}]_{33}$ and $[\hat{\boldsymbol{D}}_{\rm R}]_{33}$. The effective coefficient $[\hat{\mathscr{C}}]_{33}$ (see Remark 3) can be computed by using the analytical formula (see e.g. [56, 69]),

Parameter	Unit	Value	Parameter	Unit	Value
L	[cm]	28.000	λ_1	[Pa]	1.00
u_L	[cm]	1.0000	λ_2	[Pa]	2.00
γ	[1/s]	1.0000	μ_1	[Pa]	0.10
α	[−]	1.0035	μ_2	[Pa]	0.06
β	[−]	−0.0035	t_0	[s]	0.00
N	[−]	4.0000	t_f	[s]	10.0

Table 1: Parameters used in the numerical simulations.

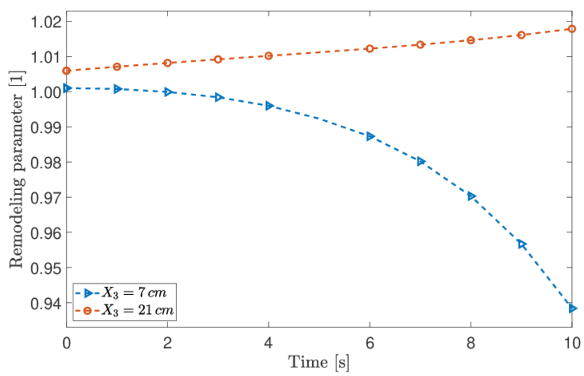

Figure 2: Evolution of the remodeling parameter p at two different points ($X_3 = 7\,\text{cm}$ and $X_3 = 21\,\text{cm}$) of the macroscopic domain.

$$[\hat{\mathscr{C}}]_{ijkl} = \langle [\mathscr{C}]_{ijkl} - [\mathscr{C}]_{ijp3}([\mathscr{C}]_{p3s3})^{-1}[\mathscr{C}]_{s3kl}\rangle \\ + \langle [\mathscr{C}]_{ijp3}([\mathscr{C}]_{p3s3})^{-1}\rangle \langle ([\mathscr{C}]_{s3t3})^{-1}\rangle^{-1} \langle ([\mathscr{C}]_{t3m3})^{-1}[\mathscr{C}]_{m3kl}\rangle. \qquad (81)$$

We observe that even if a loading ramp condition has been imposed on $\boldsymbol{u}^{(0)}$ at the border $X_3 = L$, the effective coefficient $[\hat{\mathscr{C}}]_{33}$ does not vary on time. This is because, in contrast to the case in which the plastic-like distortions are accounted for, the cell and homogenized problems (cf. (48) and (49)) are decoupled. On the other hand, the pulled-back effective coefficients $[\hat{\mathscr{C}}_{\text{R}}]_{33}$ and $[\hat{\boldsymbol{D}}_{\text{R}}]_{33}$, given by Equations (47a) and (47b), respectively, do change in time since their equations are coupled with an evolution one and, as it can be observed, they are strongly influenced by the initial distribution of p. In fact, at the spatial point $X_3 = 21\,\text{cm}$, that is, when $p > 1$, $[\hat{\mathscr{C}}_{\text{R}}]_{33}$ decreases and $[\hat{\boldsymbol{D}}_{\mathrm{R}}]_{33}$ increases with time. The contrary occurs at $X_3 = 7\,\mathrm{cm}$, i.e. when $p < 1$.

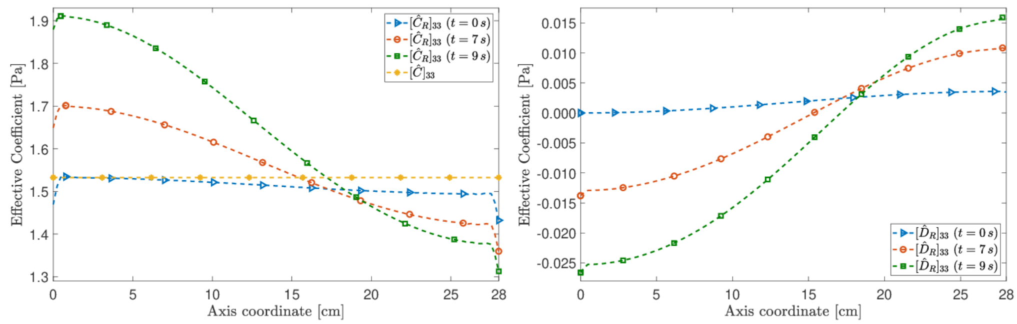

Figure 3: Spatial distribution of the effective coefficients $[\hat{\mathscr{C}}]_{33}$, $[\hat{\mathscr{C}}_{\mathrm{R}}]_{33}$ and $[\hat{\boldsymbol{D}}_{\mathrm{R}}]_{33}$ at different time instants.

Additionally, in Fig. 4 it is illustrated the third component of the macroscopic leading order term of the displacement $\boldsymbol{u}^{\varepsilon}$ at three different time instants. Particularly, we plot the numerical solution of the homogenized problems (46) and (49), represented with $[\boldsymbol{u}_{\mathrm{R}}^{(0)}]_3$ and $[\boldsymbol{u}^{(0)}]_3$, respectively. We note that, as expected from our election of the boundary condition, the displacement component increases monotonically in time. However, we notice that the introduction of the plastic-like distortions has a direct impact on the displacement distribution in the interior macroscopic points. Specifically, in these points the displacement has a higher magnitude.

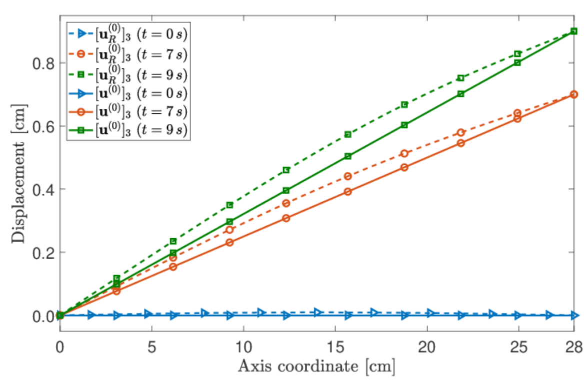

Figure 4: Spatial distribution of the macroscopic leading order term of the displacement with remodeling ($[\boldsymbol{u}_{\mathrm{R}}^{(0)}]_3$) and without remodeling ($[\boldsymbol{u}^{(0)}]_3$).

The situation described in our numerical simulations, although simplified, could be a good starting point in the study of the remodeling of biological tissues. For example, the geometrical properties of bone's osteons permit to model them as layered composites (see e.g. [69]).

8. Concluding remarks

In the present work, we studied the dynamics of a heterogeneous material, constituted by two hyperlastic media with evolving micro-structure, by the application of the asymptotic homogenization technique. The evolution of the micro-structure of the composite media was characterized through the development of plastic-like distortions, which were described by means of the BKL decomposition.

The asymptotic homogenization method was applied to a set of problems comprising a scale-dependent, quasi-static law of balance of linear momentum and an evolution law for the tensor of plastic-like distortions. After obtaining the local and homogenized problems, we rewrote them by considering the De Saint-Venant strain energy density within the limit of small deformations. Although the selection of the strain energy density was due to its simplicity, it is helpful for the description of remodeling processes undergoing small deformations. For instance, this could be the case for describing bone aging. Then, the theoretical setting developed in the present work is applicable (Elastoplasticity is actually quite appropriate to model the bone [73]). In such a case, appropriate constitutive laws describing the progression of the material properties should be found based on experimental literature (e.g. [35]). Nevertheless, for studying a larger range of problems, we need to select nonlinear constitutive laws and write the corresponding cell and homogenized problems.

As a consequence of the introduction of the tensor of plastic distortions, two independent cell problems were inferred, which reduce to the classical cell problems encountered in the homogenization of linear problems in elastostatics. Moreover, we proposed an evolution equation for the inelastic distortions describing a remodeling process. Such evolution law models a stress-driven production of inelastic distortions, as the one that is often encountered in studies of inelastic processes constructed on the decomposition given by (5) [78]. The evolution law is suitable for the case of finite strain Elastoplasticity, and for the case of remodeling of biological tissues. Finally, we outlined a computational procedure in order to solve the up-scaled problems and we performed numerical simulations for a particular case of a layered composite body. Besides, we assumed that the leading order term of the asymptotic expansion of the tensor of plastic distortions, $\boldsymbol{F}_{\mathrm{p}}^{(0)}$, depends only on the macro-scale variable X. This consideration, however, might be relaxed by allowing $\boldsymbol{F}_{\mathrm{p}}^{(0)}$ to take into account the heterogeneities of the composite material through the microscopic spatial variable Y. The numerical results showed the influence of the plastic-like distortions on both the effective coefficients and the macroscopic leading order term of the displacement.

As future work, we intend to deal with the resolution of a particular problem, like for instance the modeling of bones [49], tumor growth [67, 2, 43, 52, 70, 71], or tissue aging [20]. A further step could be the study, with the aid of the Homogenization Theory, of the coupling between the results presented in this work and the fluid flow in a hydrated tissue, or in the case of wavy laminar structures.

Acknowledgments

AR has been funded by the *Istituto Nazionale di Alta Matematica* "Francesco Saveri" (National Institute for High Mathematics "Francesco Saveri") through a research project MATHTECH-CNR-INdAM and is currently employed in the research project "Mathematical multi-scale modeling of biological tissues" (N. 64) financed by the Politecnico di Torino (Scientific Advisor: Alfio Grillo).. RR gratefully acknowledges the "Proyecto Nacional de Ciencias Básicas No. 7515, Cuba 2015–2018. JM and RP acknowledge support from the Ministry of Economy in Spain (project reference DPI2014-58885-R).

Declaration of interest

The Authors declare that they have no conflict of interest.

Article information

DOI: 10.1016/j.ijnonlinmec.2018.06.012. Available online: July 2, 2018
Journal: *International Journal of Non-Linear Mechanics* 106 (2018) 245-257

Bibliography

[1] Allaire, G., Briane, M. (1996). *Multiscale convergence and reiterated homogenisation*. Proceedings of the Royal Society of Edinburgh: Section A Mathematics 126:297-342.

[2] Ambrosi, D., Mollica, F. (2002). *On the mechanics of a growing tumor.* International Journal of Engineering Science 40:1297-1316.

[3] Ambrosi, D., Guana, F. (2007). *Stress-modulated growth.* Mathematics and Mechanics of Solids 12:319-342.

[4] Auriault, J. L., Boutin, C., Geindreau, C. (2009). *Homogenization of Coupled Phenomena in Heterogenous Media.* ISTE, London, UK; J. Wiley, New Jersey, EE. UU.

[5] Bakhvalov, N., Panasenko, G. (1989). *Homogenization: Averaging processes in periodic media.* Kluwer, Dordrecht, The Netherlands.

[6] Benveniste, Y. (2006). *A general interface model for a three-dimensional curved thin anisotropic interphase between two anisotropic media.* Journal of the Mechanics and Physics of Solids, 54(4):708-734.

[7] Benveniste, Y. and Miloh, T. (2001). *Imperfect soft and stiff interfaces in two-dimensional elasticity.* Mechanics of Materials, 33(6):309-323.

[8] Bensoussan, A., Lions, J.-L., Papanicolaou, G. (1978). *Asymptotic Analysis for Periodic Structures.* AMS Chelsea Publishing.

[9] Burridge, R., Keller, J. B. (1981). *Poroelasticity equations derived from microstructure.* The Journal of the Acoustical Society of America 70:1140-1146.

[10] Byrne, H. (2003). *Modelling avascular tumour growth* in L. Preziosi Ed. *Cancer modelling and simulations.* Chapman & Hall/CRC.

[11] Castañeda, P. P. (1991). *The effective mechanical properties of nonlinear isotropic composites.* Journal of the Mechanics and Physics of Solids 39:45-71.

[12] Cermelli, P., Fried, E., Sellers, S. (2001). *Configurational stress, yield and flow in rate-independent plasticity.* Proceedings of the Royal Society A 457:1447-1467.

[13] Ciarletta, P., Destrade, M., and Gower, A. L. (2016). *On residual stresses and homeostasis: an elastic theory of functional adaptation in living matter.* Scientific Reports, 6(1).

[14] Cioranescu, D., Donato, P. (1999). *An Introduction to Homogenization.* Oxford University Press Inc., New York, EE. UU.

[15] Collis, J., Brown, D. L., Hubbard, M. E., O'Dea, R. D. (2017). *Effective equations governing an active poroelastic medium*. Proceedings of the Royal Society A 473:20160755.

[16] Cowin, S. C. (2000). *How is a tissue built?* Journal of Biomechanical Engineering, 122(6):553.

[17] Curnier, A., He, Q.-C., Zysset, P. (1995). *Conewise linear elastic materials*. Journal of Elasticity 37:1-38.

[18] Di Carlo, A., Quiligotti, S. (2002). *Growth and balance*. Mechanics Research Communications 29:449-456.

[19] Di Stefano, S., Carfagna, M., Knodel, M. M., Hashlamoun, K., Federico S., Grillo A. *Anelastic reorganisation in fibre-reinforced biological tissues.* Submitted.

[20] Epstein, M. (2009). *The split between remodelling and aging*. International Journal of Non-Linear Mechanics 44.

[21] Epstein, M., Elżanowski, M. (2007). *Material inhomogeneities and their evolution. A geometric approach*. Springer-Verlag Berlin Heidelberg.

[22] Epstein, M., Maugin, G. A. (1996). *On the geometrical material structure of anelasticity*. Acta Mechanica 115.

[23] Epstein, M., Maugin, G. A. (2000). *Thermomechanics of volumetric growth in uniform bodies*. International Journal of Plasticity 16:951-978.

[24] Fang, Z., Yan, C., Sun, W., Shokoufandeh, A., Regli, W. (2005). *Homogenization of heterogeneous tissue scaffold: A comparison of mechanics, asymptotic homogenization, and finite element approach*. Applied Bionics and Biomechanics 2:17-29.

[25] Federico, S. (2012). *Covariant formulation of the tensor algebra of nonlinear elasticity*. International Journal of Non-Linear Mechanics 47:273-284.

[26] Ganghoffer, J.-F. (2010). *On Eshelby tensors in the context of thermodynamics of open systems: Applications to volumetric growth*. International Journal of Engineering Science 48:2081-2098.

[27] Ganghoffer, J.-F. (2013). *A kinematically and thermodynamically consistent volumetric growth model based on the stress-free configuration*. International Journal of Solids and Structures 50:3446-3459.

[28] Gei, M., Genna, F., Bigoni, D. (2002). *An Interface Model for the Periodontal Ligament*. Journal of Biomechanical Engineering, 124(5):538.

[29] Giverso, C., Preziosi, L. (2012). *Modelling the compression and reorganization of cell aggregates*. Mathematical Medicine and Biology 29:181-204.

[30] Goriely, A. (2017). *The Mathematics and Mechanics of Biological Growth*. Springer.

[31] Grillo, A., Prohl, R., Wittum, G. (2015). *A generalised algorithm for anelastic processes in elastoplasticity and biomechanics*. Mathematics and Mechanics of Solids 22:502-527.

[32] Grillo, A., Carfagna, M. Federico, S. (2018). *An Allen-Cahn approach to the remodelling of fibre-reinforced anisotropic materials*. Journal of Engineering Mathematics (In Press).

[33] Grillo, A., Federico, S., Wittum, G. (2012). *Growth, mass transfer and remodelling in fibre-reinforced multi-constituent materials*. International Journal of Non-Linear Mechanics 47:388-401.

[34] Grillo, A., Prohl, R., Wittum, G. (2016). *A poroplastic model of structural reorganisation in porous media of biomechanical interest*. Continuum Mechanics and Thermodynamics 28:579-601.

[35] Grynpas, M. (1993). *Age and disease-related changes in the mineral of bone*. Calcified Tissue International 53:57-64.

[36] Guinovart-Díaz, R., Rodríguez-Ramos, R., Bravo-Castillero, J., López-Realpozo, J., Sabina, F., Sevostianov, I. (2013). *Effective elastic properties of a periodic fiber reinforced composite with parallelogram-like arrangement of fibers and imperfect contact between matrix and fibers*. International Journal of Solids and Structures, 50(13):2022-2032.

[37] Hammer, D. A. and Tirrell, M. (1996). *Biological adhesion at interfaces.* Annual Review of Materials Science, 26(1):651-691.

[38] Hashin, Z. (1990). *Thermoelastic properties of fiber composites with imperfect interface.* Mechanics of Materials, 8(4):333-348.

[39] Hashin, Z. (2002). *Thin interphase/imperfect interface in elasticity with application to coated fiber composites.* Journal of the Mechanics and Physics of Solids, 50(12):2509-2537.

[40] Holmes, M. H. (1995). *Introduction to perturbation methods* (Vol. 20). Springer Science & Business Media, Springer-Verlag, New York.

[41] Hori, M., Nemat-Nasser, S. (1999). *On two micromechanics theories for determining micro–macro relations in heterogeneous solids.* Mechanics of Materials 31:667-682.

[42] Javili, A., Steinmann P., Kuhl, E. (2014). *A novel strategy to identify the critical conditions for growth-induced instabilities.* Journal of the Mechanical Behavior of Biomedical Materials 29:20-32.

[43] Jain, R. K., Martin, J. D., Stylianopoulos, T. (2014). *The role of mechanical forces in tumor growth and therapy.* Annual Review of Biomedical Engineering 16:321-346.

[44] Olsson, T., Klarbring, A. (2008). *Residual stresses in soft tissue as a consequence of growth and remodeling: application to an arterial geometry.* European Journal of Mechanics A/Solids 27:959-974.

[45] Kuhl, E., Holzapfel, G.A. (2007). *A continuum model for remodeling in living structures.* Journal of Material Science 42:8811–8823.

[46] Lefik, M., Schrefler, B. (1996). *Fe modelling of a boundary layer corrector for composites using the homogenization theory.* Engineering with Computers 13:31-42.

[47] Leyrat, A., Duperray, A., Verdier, C. (2003). *Cancer Modelling and Simulation*, chapter *Adhesion Mechanisms in Cancer Metastasis* Ed. L. Preziosi. Chapman & Hall/CRC Mathematical and Computational Biology.

[48] Lin, W. J., Iafrati, M. D., Peattie, R. A., and Dorfmann, L. (2018). *Growth and remodeling with application to abdominal aortic aneurysms.* Journal of Engineering Mathematics, 109(1):113-137.

[49] Lu, Y., Lekszycki, T. (2016). *Modelling of bone fracture healing: influence of gap size and angiogenesis into bioresorbable bone substitute.* Mathematics and Mechanics of Solids 22:1997-2010.

[50] Lubliner, J. (2008). *Plasticity Theory (Dover Books on Engineering).* Dover Publications.

[51] Lukkassen, D., Milton, G. W. (2002). *On hierarchical structures and reiterated homogenization.* Function Spaces, Interpolation Theory and Related Topics 355-368.

[52] Mascheroni, P., Carfagna, M., Grillo, A., Boso, D. P., Schrefler, B. A. (2018). *An avascular tumor growth model based on porous media mechanics and evolving natural states.* Mathematics and Mechanics of Solids DOI: 10.1177/1081286517711217 (In press).

[53] Marsden, J. E., Hughes, T. J. R. (1983). *Mathematical Foundations of Elasticity.* Dover Publications Inc., New York.

[54] Maugin, G. A., Epstein, M. (1998). *Geometrical material structure of elastoplasticity.* International Journal of Plasticity 14:109-115.

[55] Mićunović, M. V. (2009). *Thermomechanics of Viscoplasticity - Fundamentals and Applications.* Springer, Heidelberg, Germany

[56] Milton, G. W. (2002). *The Theory of Composites.* Cambridge University Press .

[57] Panasenko, G. (2005). *Multi-Scale Modelling for Structures and Composites.* Springer, Berlin.

[58] Parnell, W. J., Vu, M. V., Grimal, Q., Naili, S. (2012). *Analytical methods to determine the effective mesoscopic and macroscopic elastic properties of cortical bone.* Biomechanics and Modeling in Mechanobiology 11:883-901.

[59] Penta, R., Ambrosi, D. (2014). *Effective governing equations for poroelastic growing media*. Quarterly Journal of Mechanics and Applied Mathematics 67:69-91.

[60] Penta, R., Gerisch, A. (2015). *Investigation of the potential of asymptotic homogenization for elastic composites via a three-dimensional computational study*. Computing and Visualization in Science 17:185-201.

[61] Penta, R., Gerisch, A. (2017). *The asymptotic homogenization elasticity tensor properties for composites with material discontinuities*. Continuum Mechanics and Thermodynamics 29:187-206.

[62] Penta, R., Gerisch, A. (2018). *An Introduction to Asymptotic homogenization* in Gerisch, A., Penta, R., Lang., J (eds.) *Multiscale models in Mechano and Tumor Biology*, Lecture Notes in Computational Science and Engineering (122), Springer.

[63] Penta, R., Merodio, J. (2017). *Homogenized modeling for vascularized poroelastic materials*. Meccanica 52:3321-3343.

[64] Penta, R., Ramírez-Torres, A., Merodio, J., Rodríguez-Ramos, R. (2018). *Effective balance equations for elastic composites subject to inhomogeneous potentials*. Continuum Mechanics and Thermodynamics 30:145-163.

[65] Penta, R., Raum, K., Grimal, Q., Schrof, S., Gerisch, A. (2016). *Can a continuous mineral foam explain the stiffening of aged bone tissue? A micromechanical approach to mineral fusion in musculoskeletal tissues*. Bioinspiration & Biomimetics 11:035004.

[66] Persson, L. E., Persson, L., Svanstedt, N., Wyller, J. (1993). *The homogenization method. An introduction.* Studentlitteratur, Lund.

[67] Preziosi, L., Vitale, G. (2011). *A multiphase model of tumor and tissue growth including cell adhesion and plastic reorganization*. Mathematical Models and Methods in Applied Sciences 21:1901-1932.

[68] Pruchnicki, E. (1998). *Hyperelastic homogenized law for reinforced elastomer at finite strain with edge effects*. Acta Mechanica 129:139-162.

[69] Ramírez-Torres, A., Penta, R., Rodríguez-Ramos, R., Merodio, J., Sabina, F. J., Bravo-Castillero, J., Guinovart-Díaz, R., Preziosi, L., Grillo, A. (2018). *Three scales asymptotic homogenization and its application to layered hierarchical hard tissues*. International Journal of Solids and Structures 130-131:190-198.

[70] Ramírez-Torres, A., Rodríguez-Ramos, R., Merodio, J., Bravo-Castillero, J., Guinovart-Díaz, R., Alfonso, J. C. L. (2015). *Action of body forces in tumor growth*. International Journal of Engineering Science 89:18-34.

[71] Ramírez-Torres, A., Rodríguez-Ramos, R., Merodio, J., Bravo-Castillero, J., Guinovart-Díaz, R., Alfonso, J. C. L. (2015). *Mathematical modeling of anisotropic avascular tumor growth*. Mechanics Research Communications 69:8-14.

[72] Reimer, P., Parizel, P. M., Meaney, J. F. M., Stichnoth, F. A., editors (2010). *Clinical MR Imaging*. Springer Berlin Heidelberg.

[73] Ritchie, R. O., Buehler, M. J., Hansma, P. (2009). *Plasticity and toughness in bone*. Physics Today 62:41-47.

[74] Rohan, E., Cimrman, R., Lukeš, V. (2006). *Numerical modelling and homogenized constitutive law of large deforming fluid saturated heterogeneous solids*. Composites and Structures 84:1095-1114.

[75] Rohan, E., Lukeš, V. (2010). *Microstructure based two-scale modelling of soft tissues*. Mathematics and Computers in Simulation 80:1289-1301.

[76] Rodriguez, E. K., Hoger, A., McCulloch, A. D. (1994). *Stress-dependent finite growth in soft elastic tissues*. Journal of Biomechanics 27:455-467.

[77] Sanchez-Palencia, E. (1980). *Non-homogeneous media and vibration theory*. In: Lecture Notes in Physics, 127. Springer-Verlag, Berlin.

[78] Simo, J. C., Hughes, T. J. R. (1988). *Computational Plasticity*. Springer, New York.

[79] Suquet, P. (1987). *Elements of homogenization for inelastic solid mechanics* in *Homogenization techniques for composite media*. Eds. E. Sanchez-Palencia and A. Zaoui. Springer-Verlag, Berlin.

[80] Taber, L. A. (1995). *Biomechanics of growth, remodeling, and morphogenesis*. Applied Mechanics Reviews, 48(8):487.

[81] Taffetani, M., de Falco, C., Penta, R., Ambrosi, D., Ciarletta, P. (2014). *Biomechanical modelling in nanomedicine: multiscale approaches and future challenges*. Archive of Applied Mechanics 84:1627-1645.

[82] Telega, J. J., Galka, A., Tokarzewski, S. (1999). *Application of the reiterated homogenization to determination of effective moduli of a compact bone*. Journal of Theoretical and Applied Mechanics 37(3):687-706.

[83] Tsalis, D., Baxevanis, T., Chatzigeorgiou, G., Charalambakis, N. (2013). *Homogenization of elastoplastic composites with generalized periodicity in the microstructure*. International Journal of Plasticity 51:161-187.

[84] Walpole, L. J. (1981). *Elastic behaviour of composites materials: theoretical foundations*. Advances in Applied Mechanics 21:169-242.

[85] Walpole, L. J. (1984). *Fourth-rank tensors of the thirty two crystal classes: multiplication tables*. Proceedings of the Royal Society A 391:149-179.

[86] https://en.wikipedia.org/wiki/plasticity (physics)